ANALYSIS OF PALEOCURRENT DIRECTIONS OF SEDIMENTARY ROCKS USING ANISOTROPY OF MAGNETIC SUSCEPTIBILITY (AMS) FROM TALCHIR AND BARAKAR FORMATIONS IN DAMODAR VALLEY

THESIS SUBMITTED FOR THE PARTIAL FULFILMENT OF THE DEGREE OF MASTER OF SCIENCE (APPLIED GEOLOGY) OF JADAVPUR UNIVERSITY

By

SOLANKY DAS

ROLL No.: MGEO194030

DEPARTMENT OF GEOLOGICAL SCIENCES
JADAVPUR UNIVERSITY
KOLKATA

2019

ANALYSIS OF PALEOCURRENT DIRECTIONS OF SEDIMENTARY ROCKS USING ANISOTROPY OF MAGNETIC SUSCEPTIBILITY (AMS) FROM TALCHIR AND BARAKAR FORMATIONS IN DAMODAR VALLEY

THESIS SUBMITTED FOR THE PARTIAL FULFILMENT OF THE DEGREE OF MASTER OF SCIENCE (APPLIED GEOLOGY)
OF
JADAVPUR UNIVERSITY

By

SOLANKY DAS

ROLL NO: MGEO194030

DEPARTMENT OF GEOLOGICAL SCIENCES
JADAVPUR UNIVERSITY
KOLKATA

2019

যাদবপুর বিশ্ববিদ্যালয়
কলকাতা-৭০০ ০৩২, ভারত

JADAVPUR UNIVERSITY
KOLKATA-700 032, INDIA

FACULTY OF SCIENCE : DEPARTMENT OF GEOLOGICAL SCIENCES

This is to certify that **MISS SOLANKY DAS** worked under my guidance on the topic entitled **"ANALYSIS OF PALEOCURRENT DIRECTIONS OF SEDIMENTARY ROCKS USING ANISOTROPY OF MAGNETIC SUSCEPTIBILITY (AMS) FROM TALCHIR AND BARAKAR FORMATIONS IN DAMODAR VALLEY"** in the Department of Geological Sciences. She has completed her work, which is being submitted herewith as a thesis towards partial fulfilment of her **M. Sc. Degree Examination in Applied Geology (2019)** of Jadavpur University.

Name of Supervisor

1. Prof. Supriya Mondal

Signature of Supervisor

Supriya Mondal
30/05/19

Dr. Supriya Mondal
PROFESSOR
Department of Geological Sciences
JADAVPUR UNIVERSITY
Kolkata-700 032, India

30-05-2019
Head of the Department
Department of Geological Sciences
Jadavpur University
Kolkata-700032, India

Head
Department of Geological Sciences
Jadavpur University
Kolkata-700032

Website : www.jadavpur.edu
E-mail : hod_geological@jdvu.ac.in
Phone : 2414 6666 Extn. 2268

CONTENTS

ACKNOWLEDGEMENTS i

ABSTRACT ii

Chapter: 1 INTRODUCTION 1

Chapter: 2 BACKGROUND GEOLOGY AND SAMPLE COLLECTION 4

Chapter: 3 PETROGRAPHY AND MINERALOGY 9

- Petrography
- Magnetic Mineralogy

Chapter: 4 ANISOTROPY OF MAGNETIC SUSCEPTIBILITY STUDY 23

- Introduction
- Magnetic Fabric
- Susceptibility Ellipsoids and Parameters
- Methodology and Instruments used for measuring the Anisotropy of Magnetic Susceptibility
- Usefulness of AMS Study in Sedimentary Rocks
- Plotting of AMS data

Chapter: 5 RESULTS AND DISCUSSIONS 36

Chapter: 6 CONCLUSION 39

REFERENCES 40

ACKNOWLEDGEMENTS

I would like to acknowledge my supervisor Prof. SupriyaMondal, Department of Geological Sciences, Jadavpur University, for guiding me throughout my thesis work.I am also thankful to the Research Scholars Mr.Saurodeep Chatterjee and Mr. Debesh Gain for their enormous help during the petrographic study and AMS study.

[SOLANKY DAS]

ABSTRACT

Magneto-mineralogy and Anisotropy of Magnetic Susceptibility (AMS) data of rocks from Lower Gondwana succession, Damodar Valley, Maithon region, are investigated to determine the paleocurrent direction of sedimentary formations using the magnetic fabrics. The main aims of this work are to study the magneto mineralogical characters of rocks and to investigate the behaviours of Magnetic Fabrics of the studied rocks using Anisotropy of Magnetic Susceptibility (AMS) data.

The studied rock samples do not exhibit any evidence of high temperature oxidations of Fe-Ti oxides. Considering the textural relationship in rocks from different sampling sites, at least three generations of ferromagnetic mineral assemblage are distinguishable. The earliest one is the primary homogeneous titanomagnetite suffering different stages of low temperature oxidations. These are medium sized irregular grains occurring separately or associated with silicate grains. The second generation consists of Ultra-fine grains of hematite and pigmentary hematite. The last generation is the ultra-fine grains or droplets of secondary magnetite occur along the grain boundary of silicate minerals. This type of secondary magnetite can be generated during long term diagenesis processes after deposition.

All the features are suggested that the studied rocks exhibit some important magnetic signatures, which will be more useful for the identification palaeo-pole positions to fix the Damodar Valley in Gondwana time. So these types of studied rocks must be the suitable samples for the through palaeomagnetic measurements by which we can construct the APWPs of the continental blocks to unravel tectonic history of Gondwana Successions in India. The results derived from the statistical parameters (especially the q-factor), the shapes of the susceptibility ellipsoids and directional data of the AMS indicate that the magnetic fabrics within the studied units are primary (depositional) and are correlatable form the paleoenvironmental features. The orientation of the maximum (K_1), intermediate (K_2) and minimum (K_3) susceptibility axes is dispersed on the lower hemisphere equal area diagram rather than strong clusters which is not because of secondary (tectonic) influence but due to the moderate to high energy environment of deposition of the sediments in the studied units. Based on the q-factor (which is 0.581 <0.7), it is suggested the AMS indicates that the imbrication of the K_1axis is the indicator of paleocurrent. Also, the magnetic foliation (average value = 1.255) exceeds the magnetic lineation (average value = 1.107) and the shape parameter exceeds 0 in most cases pointing towards an oblate fabric. However, apart from this precise paleocurrent direction, there exists a certain degree of randomness of the susceptibility axes which are very clear indication of corresponding depositional environments.

Keywords: AMS, Fe-Ti oxide, Gondwana, Paleocurrent, Sedimentary deposition

CHAPTER: 1

INTRODUCTION

The low-field Anisotropy of Magnetic Susceptibility (AMS) technique is increasingly used in geological sciences to study the magnetic fabrics in igneous, sedimentary and metamorphic rocks (Nagata 1961; Rees 1965; Elwood 1980; Knight and Walker 1988; Tarling and Hrouda 1993; Borradaile and Henry 1997; Canon-Tapia 2004). Ising (1942) and Graham (1954) were the first to propose the application of AMS in geological studies, since then it emerged as a successful tool in determining the petrofabric and paleocurrent directions of unconsolidated sediments and sedimentary rocks (Jackson 1991; Schieber and Ellwood 1993; Park et al., 2000; Baas et al., 2007; Pare's et al., 2007; Veloso et al. During the deposition of sediments, the magnetic particles (ferrimagnetic, paramagnetic and diamagnetic) align to ambient geomagnetic field at that time, which is not isotropic and varies with directions, grain size, shape and preferred orientation (Tarling and Hrouda, 1993). The results of AMS usually represented by second-rank tensor, which can be depicted as an ellipsoid with mutually perpendicular principle axes i.e., $K1 \geq K2 \geq K3$ representing maximum, intermediate and minimum susceptibility axes respectively (Rochette et al., 1992).

In the present study, the AMS results obtained from the Gondwana sediments in the Damodar Valley. Northeast India, should be presented to understand the magnetic fabrics and their paleocurrent direction. This study, therefore, attempts for the first time to use AMS, to determine the paleocurent direction for the Gondwana Sediments from the Damodar Valley, Northeast India.

Gondwana Basins of India occur within the suture zones of Precambrian Cratonic blocks of Peninsular India along some linear belts. More than 99% of the total coal resource of the country is present within these basins. The basins are demarcated by boundary faults having graben or half-graben geometry.

These basins preserve a thick sedimentary pile deposited over nearly 200 million years from latest Carboniferous to Lower Cretaceous. However, due to lack of well constrained data, age of most of the formations is assigned tentatively. This has resulted in diversified views on both intra- and inter-basinal stratigraphic correlation particularly in case of Upper Gondwana formations.

The physical properties of bottom-current flow recorded by deep-sea sediments can provide information about the evolution of oceanic currents, their strength and direction; information on this latter point forms the basis of this contribution. Specifically, details regarding the ACC (Antarctic Circumpolar Current) significantly affect our understanding of late Cenozoic paleo oceanography, as it is thought to isolate Antarctica from the warmer waters to the north.

The **Anisotropy of Magnetic Susceptibility (AMS)** provides a gauge for sediment fabric that senses the degree of preferred grain orientation in sediments and, hence paleocurrent strength and direction. However, these results cannot be placed in a geographic context from core analysis without the use of paleomagnetic data.

Previous workers have applied AMS to sediment samples to determine relative current strength (Ellwood and Ledbetter, 1977, 1979; Ellwood et al., 1979; 1998, 2004; Hassold et al., 2006), but few have applied this method to determine paleo-directions of current flow in sediments (e.g., Ledbetter and Ellwood, 1980; Liu et al., 2001). The high sedimentation rates and high concentration of terrigeneous material at the drifts along the Antarctic Peninsula (Hassold, 2006 Chapters 3 and 4) present an opportunity to explore this potentially powerful aspect of fabric study.

So, the objectives of this work are:

1. **To study the magneto mineralogical characters of rocks of Barakar Formation in Damodar Valley.**
2. **To indentify the palaeocurrent direction using Anisotropy of Magnetic Susceptibility (AMS) data.**

The study of Anisotropy of Magnetic Susceptibility has been carried out in parallel with the ore microscopic study on Fe-Ti oxides. A detailed study has been made on the magnetic mineralogy in order to identify not only the carriers of magnetization but also to get information for analysis of the paleocurrent direction in the rocks of Barakar Formations. In most cases it is difficult to determine which particular phase of magnetic mineral is the carrier of an observed remnant component because there are typically several methods of occurrence of the same mineral in the altered and after-diagenesis rocks. Polished-thin sections were studied under microscope for the identification of the magnetic minerals and their textures and their textural relationships with the silicate minerals.

CHAPTER: 2

BACKGROUND GEOLOGY AND SAMPLE COLLECTION

2.1 Background Geology:

The covered area is basically composed of Amphibolite Gneiss (metaigneous) and sedimentary rocks. The rocks are mainly aligned towards North-East. The rock in Maithon and in adjacent area belongs to Chotonagpur gneissic complex of eastern India. The Chotonagpur gneissic complex consists of mainly Precambrian gneiss of different variety (amphibolite gneiss and granite), with some sporadic outcrop of ultramafic and basic intrusive. The Gondwana rocks are of much younger age and occurred with a linear pattern having E-W trend. The Chotonagpur gneissic complex terrain bordered by Singhbhum tectonic belt at the north of Gangatic alluvial plain at north and east. The studied area is consisting of both the Precambrian rocks and Gondwana Sediments. Our work of interest is concentrated only on Gondwana Sedimentary rocks.

Amphibolite and Amphibolite gneiss were found in the North and Northwest region of Barakar River. The East and North-East part of the top sheet is composed of metamorphic rock (predominantly amphibolite gneiss). The major rock types along the River behind the Kalyaneswari temple are Amphibolite gneiss, Granitic gneiss. The two types of rocks were interbanded. Near the meeting point of the nalah and the Barakar river we observed Gondwana succession starting with Talchir. Then the Barakar layer is exposed in the coal mine region.

2.2 Tectonic Settings:

The name Gondwanaland refers to the former supercontinent proposed by Alex du Toit (1937) and considered to be constituted of all the Southern Hemisphere continents including India. The Gondwanaland masses show evidence of similar climatic conditions and distribution of deposits from Upper Carboniferous to Jurassic times. The era began with a glacial climate producing deposits commencing with glacial boulder beds, overlying striated pavements which have been recognized in all the above-mentioned landmasses. The glacial condition was followed by fluviatile or lacustrine deposition marked with intercalated plant remains which were ultimately compressed and lithified to form extensive coal seams. The basins of the deposition must have been shallow and slowly oscillating because the cycle of deposition starting with coarse sandstones and proceeding through shales to coal seams is extensively developed. The geology of the Gondwana formations which has been extensively studied by a large number of scientists and has been published in various Records, Memoirs of GSI and journals (e.g, Fox, 1931, Pascoe, 1959, Wadia, 1961, Robinson, 1967, Mitra et al 1971).

The rocks forming this Gondwana group are largely fluviatile or lacustrine in nature and were deposited in a series of large river or lake basins which subsided due to fault movements amidst the ancient rocks. It is due to this down faulting into the Precambrian Shield that we owe the preservation of the bulk of the Gondwana strata with their rich coal seams in India.

The Gondwana formations of the Indian Peninsula occur along the relatively restricted strips and patches lying unconformably on the Precambrian basement rocks comprising chiefly granites, mica-schists, and amphibolites. The foliation planes in the basement have a high dip but their strikes vary locally from almost E-W in the south-eastern part to NE-SW in south-west and WNW-ESE in the north. The Gondwana rocks are mainly developed along two sides of a great triangular area, the third side of which is formed by the northern part of east coast of the Peninsula, i.e., from the Godavari valley to the Rajmahal Hills.

2.3 Stratigraphy:

Depositional pattern in individual basins shows wide variation. In the Damodar Valley, the succession is dominated by arenaceous facies in majority of the basins and formational contacts are blurred due to absence of marker bed and close similarity of litho character. In many basins only Barakar Formation was earlier distinguished separately from the post-Talchir strata, that too only because of its coal content, while the overlying lilho-packs deposited over unusually long time period, were often clubbed under a single name like Pali (in Sun Valley), Kamthi (in Mahanadi, Wardha, Godavari) etc. The stratigraphic succession of Gondwana Formations in DamodarValley is shown in Table 2.1 .

Table: 2.1 STRATIGRAPHIC SUCCESION OF GONDWANA BASIN IN DAMODAR VALLEY, INDIA

AGE	DAMODAR VALLEY
LOWER CREATACEOUS	
JURASSIC UPPER MIDDLE LOWER	
TRIASSIC UPPER	SUPRA PANCHET FM./ MAHADEVA FM.

~~ **UNCONFORMITY** ~~~~~~~~~~~~~~~~~~~	
MIDDLE LOWER	 PANCHET FM.
PERMIAN UPPER MIDDLE LOWER	 RANIGANJ FM. BARREN MEASURE FM. BARAKAR FM. KAHARBARI FM.
UPPER CARBONIFEROUS	TALCHIR FM.
~~ **UNCONFORMITY** ~~~~~~~~~~~~~~~~~~~	
PRECAMBRIAN BASEMENT	

****** FM- Formation**

2.4 Sampling Methods:

Extensive geological field work has been carried out to collect the systematic oriented block samples of various kinds of sedimentary rocks during field work in and around Maithon. Samples were collected in the form of Blocks using Hammer and Chisel and Magnetic Compass. Samples were distributed over surface outcrops as rock exposures of different varieties. The samples were sliced in specific thickness from the blocks for the preparation of thin sections as well as polished sections. The thin sections were studied under petrological microscopy and the polished sections were studied under the Reflected Light Microscopy. The oriented samples were then sliced to cubes having 2.2 cm. length by rock cutting machine in the laboratory for AMS measurements by Bartington Susceptibility Meter (MS2).

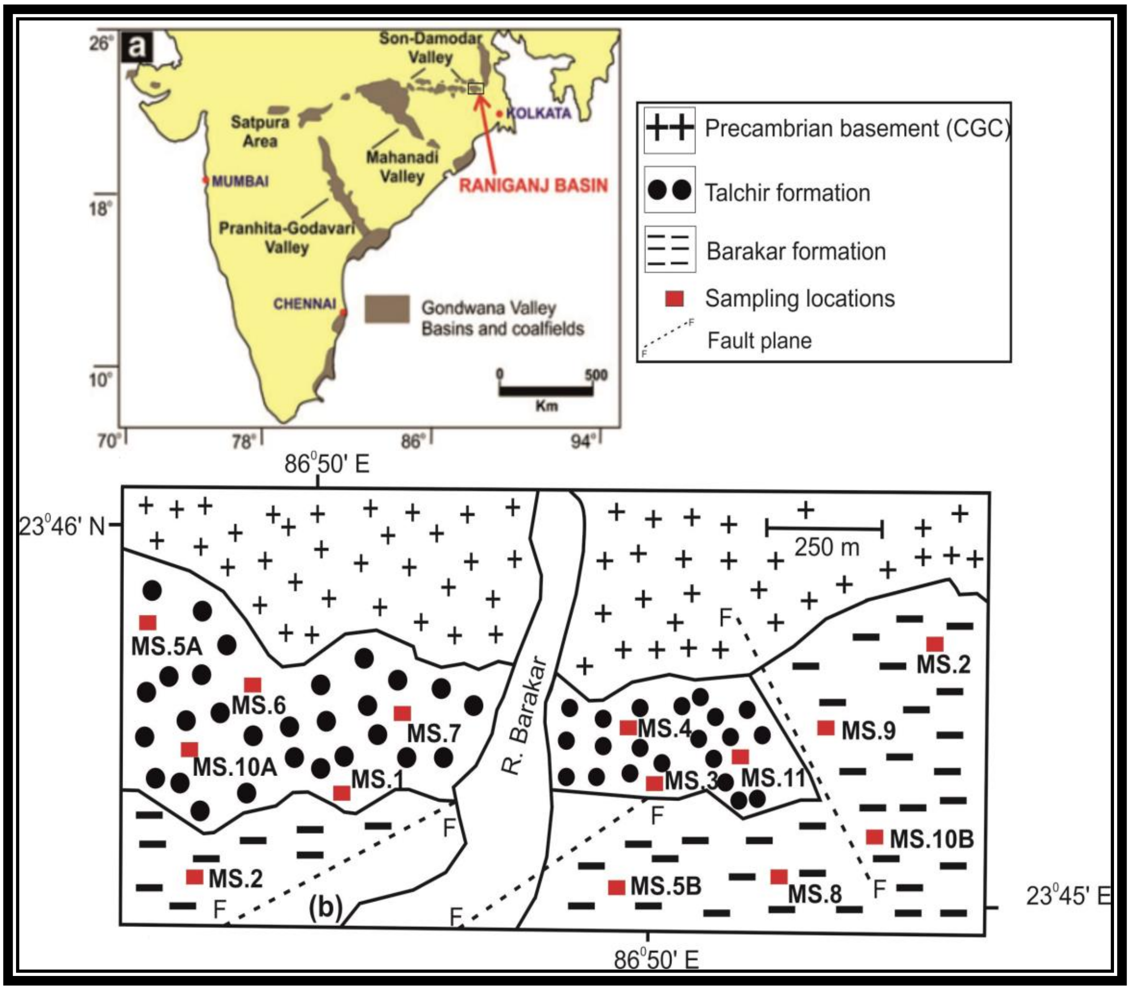

Fig. 2.2 Generalised Geological Map to plot the locations around Maithon, Jharkhand

CHAPTER: 3

PETROGRAPHY ANDMINERALOGY

3.1. Petrography:

The rock samples from Barakar Formation are generally containing quartz, feldspar, mica and opaque minerals as terrigenous constituents. These are supported by the proto-matrix formed by chert, chlorite or sericite with patches of reddish iron-oxide cement. The quartz grains are predominantly mono-crystalline and non-undulatory with a few polycrystalline quartz grains in the Talchir samples. Detrital feldspar grains are essentially microcline and un-twinned. K-feldspar and are distributed in the matrix.

The K-feldspar are fresh to completely kaolinised may be observed in majority of the samples. Some of the altered feldspars are highly pitted along with dissolved grain boundaries. This may indicate that mineral dissolution is controlled both by surface reactions and diffusion through alteration products. Altered feldspar grains sometimes show integration of numerous contraction cracks indicating post-depositional dehydration effects. Alteration of feldspar is wide spread in the biotite-rich sandstones where the replacement proceeded along the edges of the cleavage planes of biotite. Sericitization is strictly confined within the feldspar grains and from textural features it appears that the feldspar alteration occurred at least in two phases; one syn-depositional or inherited at the basin area and other is post depositional (Fig. 3.4). Primary biotite grains are aligned in preferred directions (Fig. 3.1, 3.2).

The clastic micas predominantly biotite, are present as rock fragments. Biotite grains showing brown pleochroism and straight extinction, are variably deformed, broken or torn out (Fig. 3.5, Fig. 3.6) and often bleached or may show effect of partial to complete chloritization. Biotite occur as flakes and as elongated grains often swathing around quartz grains and at places appearing to be cut across by the latter at the pressure solution contacts. Opaues also occur in association with them (Fig. 3.9). Stages of differential alteration registered in biotite grains are evidence of the prolonged diagenetic processes experienced by the rocks of Barakar Formations (Fig. 3.3).

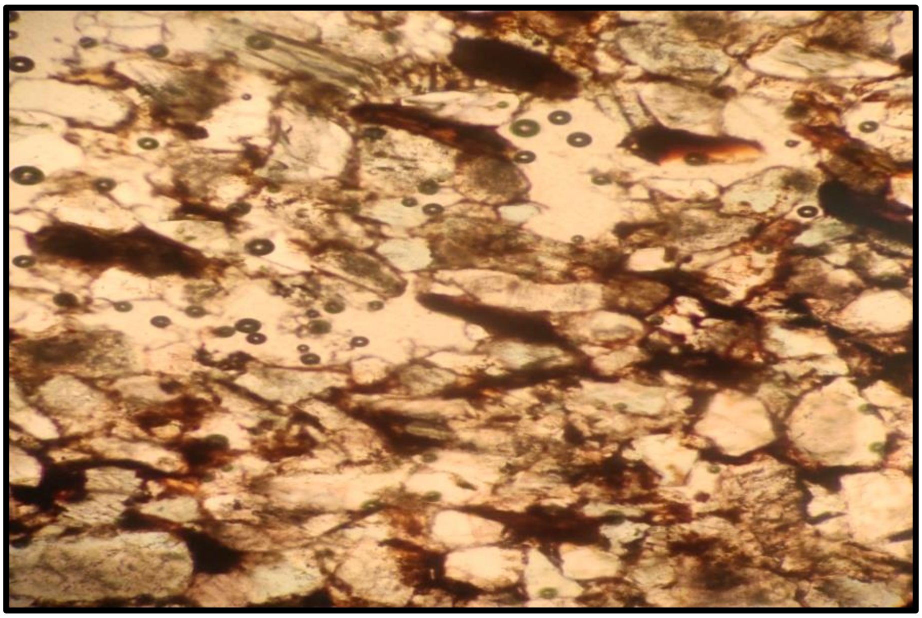

Figure 3.1. Photomicrograph of biotite oriented within framework (PPL, 200x)

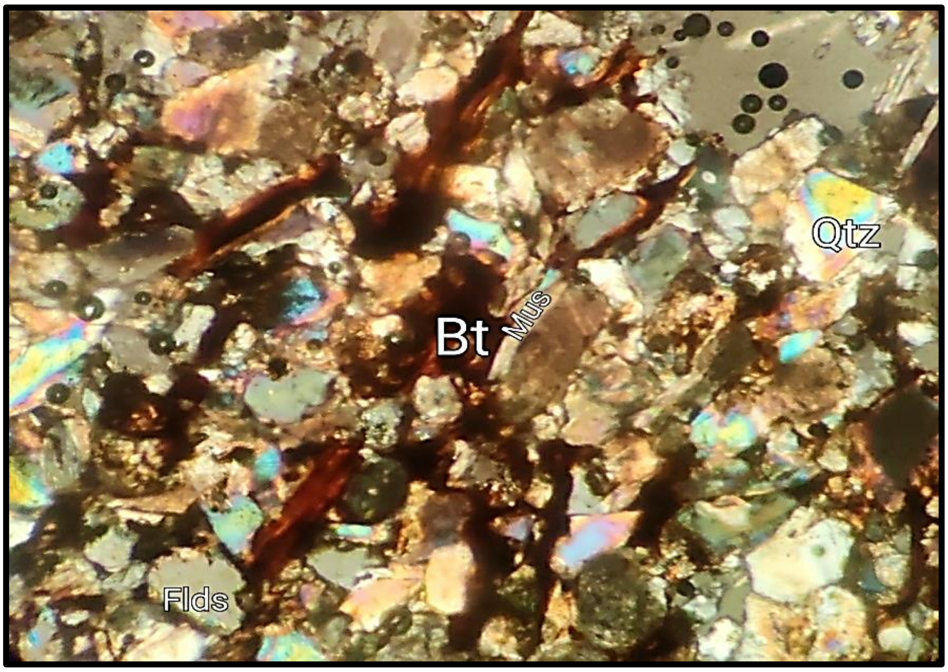

Figure 3.2. Photomicrograph of biotite and muscovite oriented within framework (XPL, 200x).

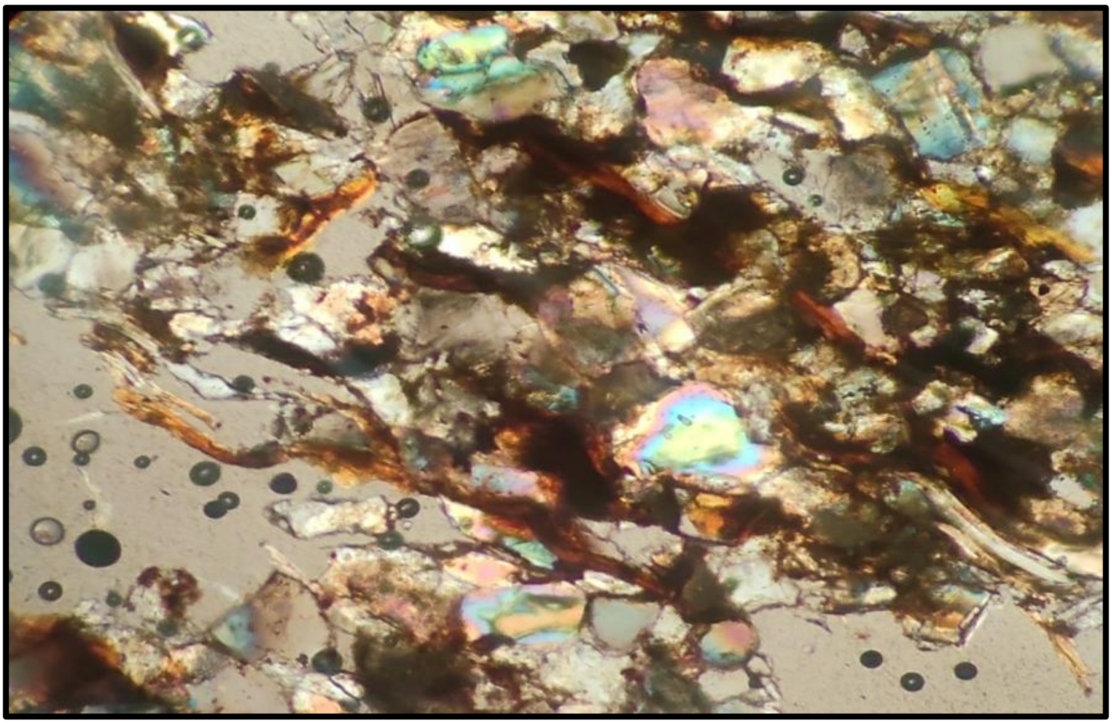

Figure 3.3 Biotite along the weak planes within framework (XPL, 200x).

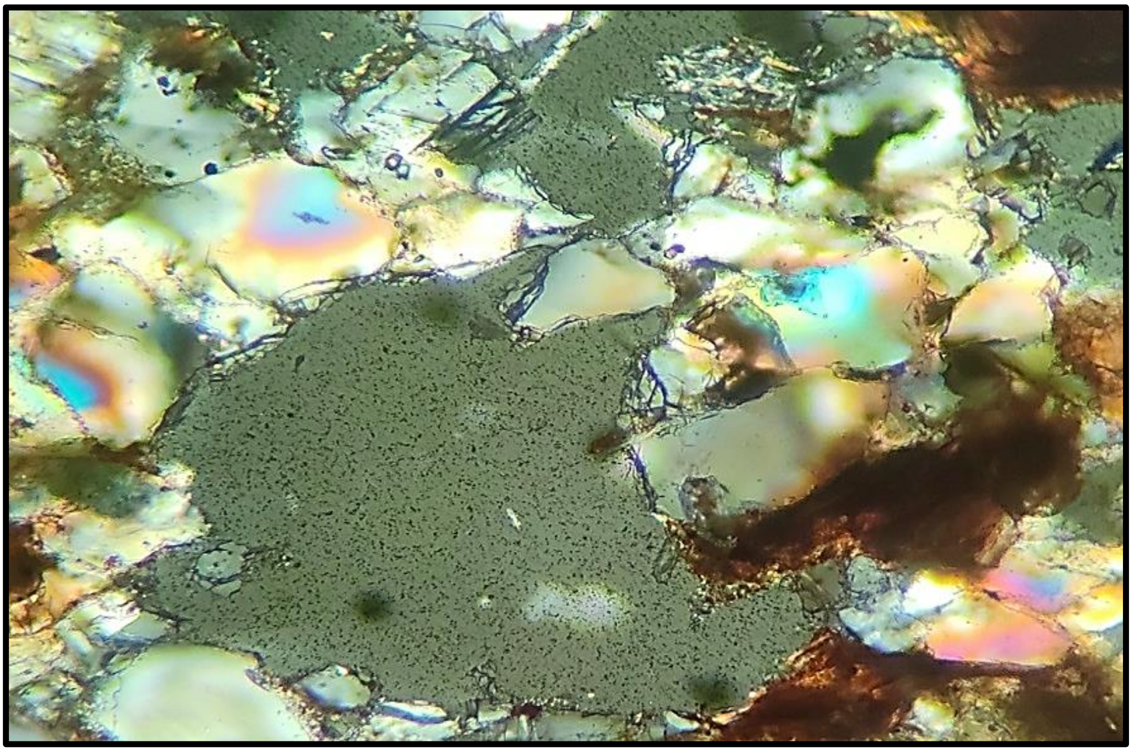

Figure 3.4. Crushing of framework grains along boundaries of fresh feldspar grains

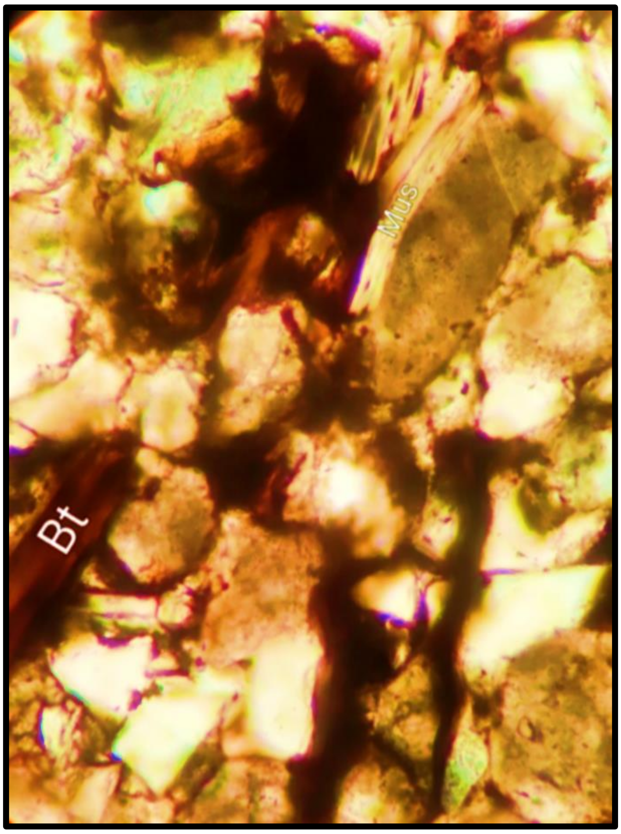

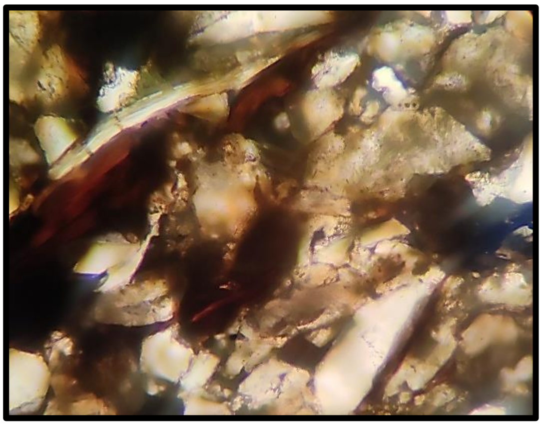

Figure 3.5. Deformed secondary biotite grains in the matrix (CPL, 200x)

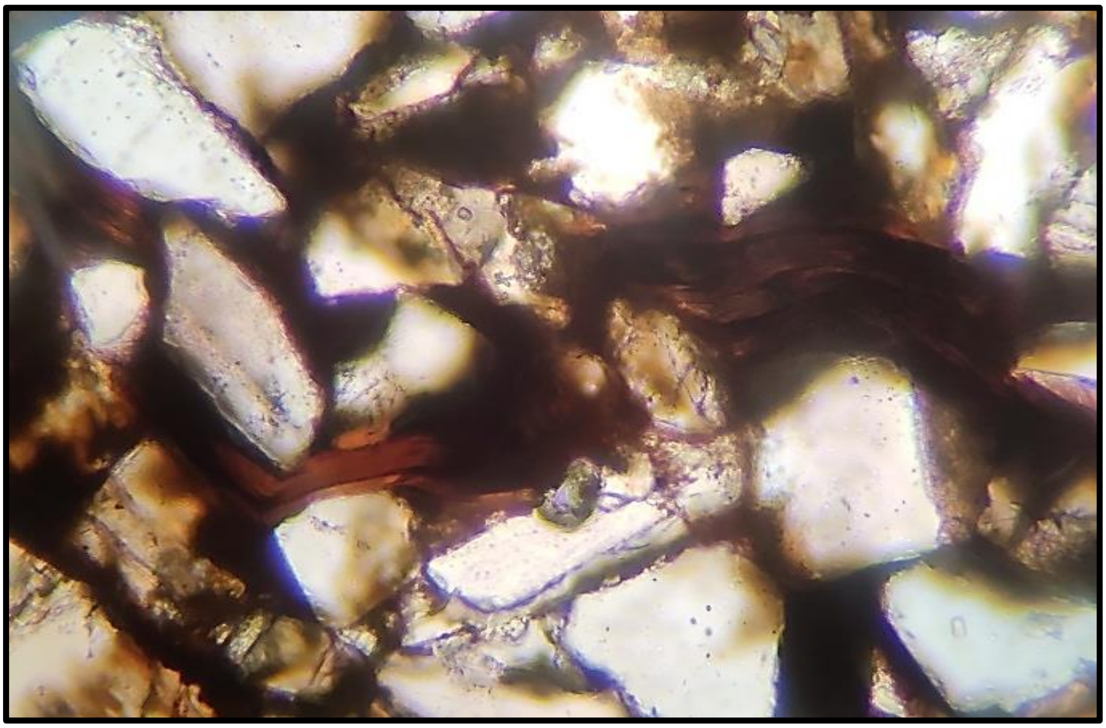

Figure 3.6. Deformed secondary biotite grains in the matrix (CPL, 200x)

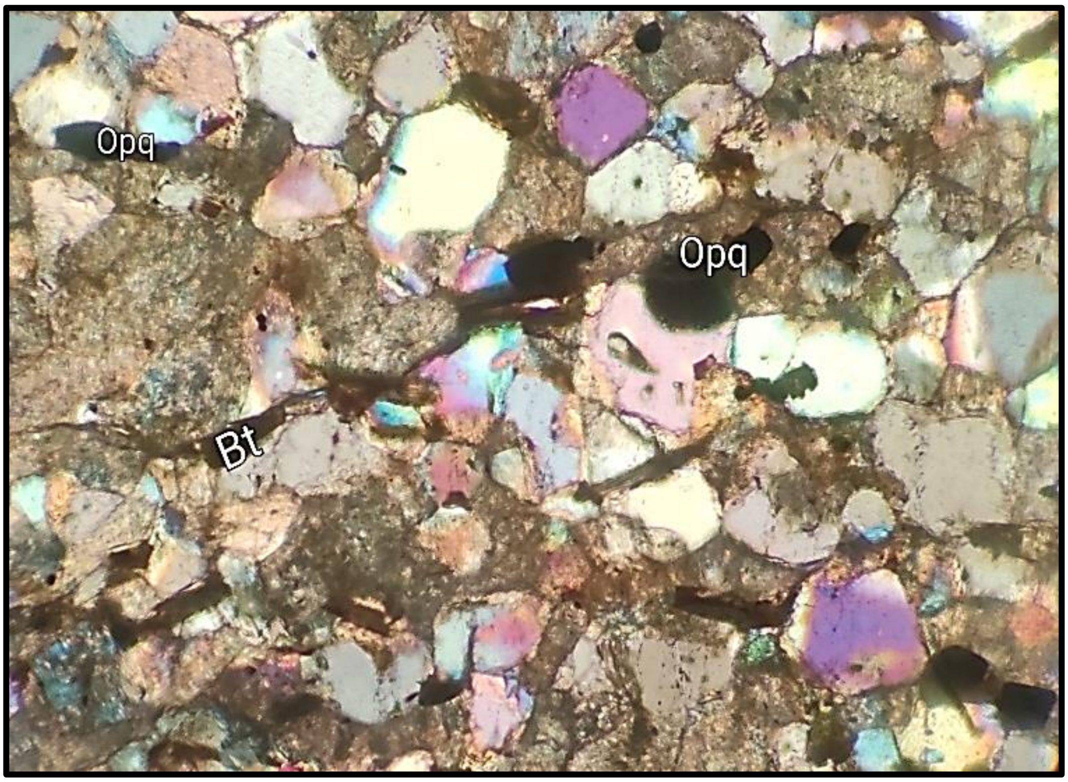

Figure 3.7. Variable occurrences of opaque minerals (XPL, 200x)

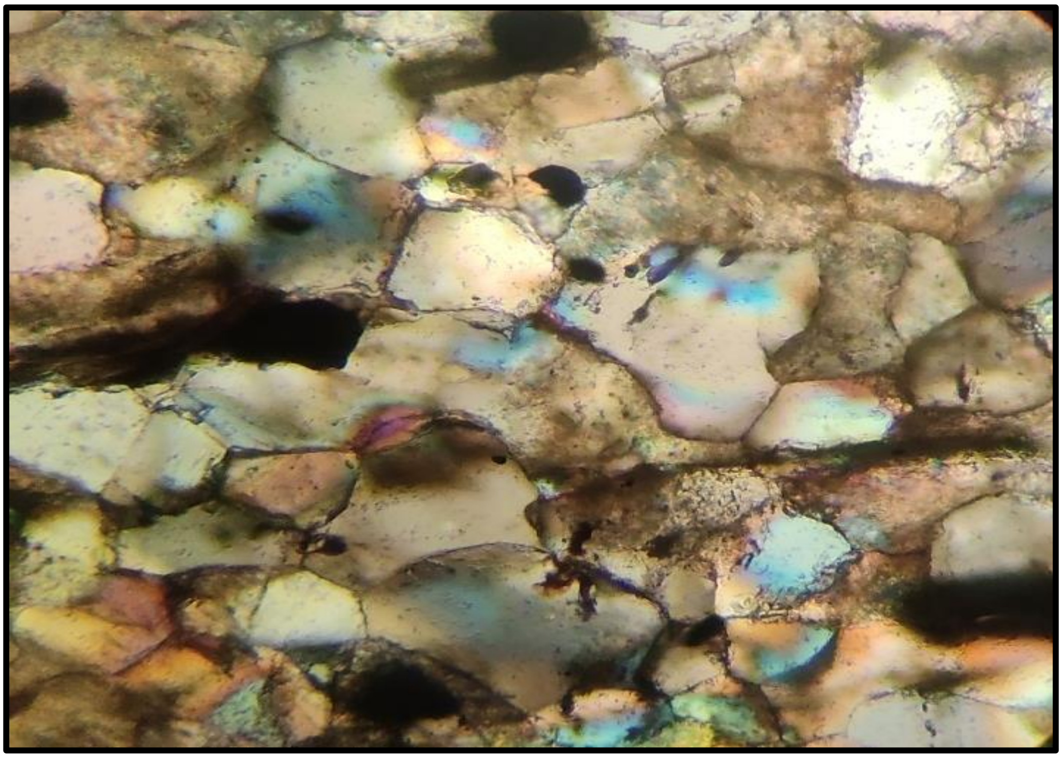

Figure 3.8. Variable occurrences of opaque minerals (XPL, 200x)

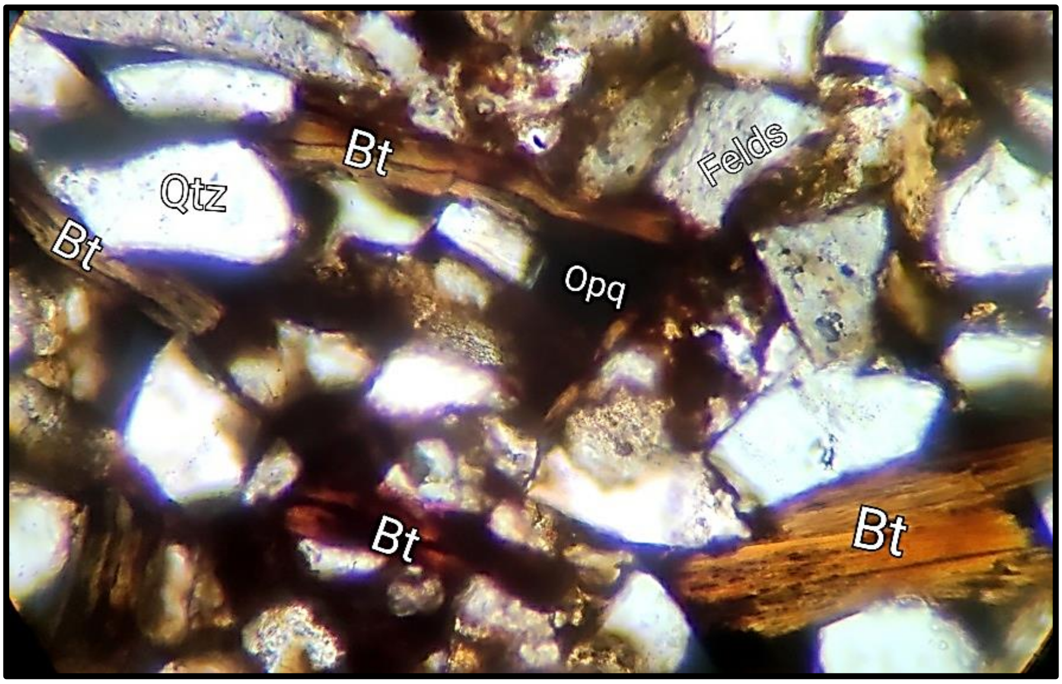

Figure 3.9. Growth of opaque minerals along the cleavage planes of altered biotite grains, CPL, 500X

3.2. Magnetic Mineralogy:

3.2.1. Generations of Fe-Ti Oxides:

A rock should be regarded as a heterogeneous assemblage of minerals, ferromagnetic, paramagnetic and diamagnetic, each grain of which makes its own contribution to the total susceptibility. The most important factors influencing rock magnetism are the type of magnetic minerals, its grain size, and the manner in which it acquires a remanent magnetization. The most important magnetic minerals are Iron-oxides and Iron-Titanium oxides. Iron-oxide minerals constitute the major opaque oxides in the different rocks from Damodar Valley region, in and around Maithon. The magnetic properties of various sedimentary rocks such as sandstone, shale, siltstones and the other rocks are found mainly as a function of their primary Fe oxide minerals and the subsequent changes during diagenesis. So, the primary Fe oxide mineralogy plays an important role in the field of sedimentary deposition and the subsequent rock formation.

Two different types of oxidation of titanomagnetite can be distinguished under ore microscopy studies, depending upon temperature and corresponding pressure.

A. First, High Temperature Oxidation that occurs above 600°C and,

B. Second, Low Temperature Oxidation that occurs about 350°C or below that temperature.

A. High Temperature Oxidation of Fe-Ti Oxides:

Two different textural assemblage of Fe-Ti oxide minerals develop from the oxidation of titanomagnetite:

a. "Oxidation-exsolution" (Buddington and Lindsley, 1964) or "exsolution" lamellae of ilmenite along (111) parting planes in titanomagnetite, which is, called trellis ilmenite (Buddington and Lindsley, 1964).

b. Post "exsolution" pseudomorphic-oxidation products rutile, titanomagnetite and pseudobrookite.

Both the assemblages develop above 600°C but at the different oxygen fugacities. Ilmenite, which is produced by oxidation-exsolution, is structurally controlled within the titanomagnetite host. With more intense oxidation the titanomagnetite host is gradually depleted in the ulvospinel component as larger concentrations of ilmenite development. The exsolved ilmenite continues to follow the path of oxidation without any dramatic effects on the titanomagnetite host. A saturation point is finally reached, which results in the exsolution of Pleonaste solid solutions and with the oxidation of the residual titanomagnetite to titanohematite.

Haggerty (1976) has classified the stages of high temperature oxidation. The letter "C" prefixes each stages of oxidation resulting from Cubic phase:

C1 Stage: Optically homogeneous titanomagnetite solid solutions enriched with Ulvospinel.

C2 Stage: Titanomagnetite having the small number of "exsolved" ilmenite lamellae along (111) crystallographic plane.

C3 Stage: Titanomagnetite with densely crowded "exsolved" ilmenite lamellae along (111) crystallographic plane.

C4 Stage: Mottling of lamellar ilmenite – intralamellartitanomagnetite intergrowth and development of ferri-rutile in metailmenite lamellae.

C5 Stage: Rutile and titanohematite extensively develop within the metailmenite lamellae and rutile-titanohematite assemblages develop incipiently within the titanomagnetite.

C6 Stage: The incipient pseudobrookite forms during this stage and three

phase assemblages, rutile, pseudobrookite and exsolved spinel develop with or without unoxidized titanomagnetite.

C7 Stage: Pseudobrookite$_{(S\ S)}$ and hematite$_{(S\ S)}$ coexist with this stage of oxidation.

In the studied sample we don't get any evidence of high temperature oxidations of Fe-Ti oxides in Gondwana Sediments.

B. Low-Temperature Oxidation of Fe-Ti Oxides:

The effects of low temperature oxidation are quite different from those of the high temperature oxidation. At the time of low temperature oxidation, the titanomagnetites have cation deficiency and due to the increase of cation deficiency in the titanomagnetite-spinel lattice with increasing degree of low temperature oxidation ultimately results in the formation of monophasic nonstoichiometric cation deficient spinel, called titanomaghemite (γ-Fe_2O_3).

This process of oxidation is known as "Maghemitization". It has been demonstrated that low temperature oxidation promotes migration of Fe-ions out of the titanomagnetite-spinel lattice resulting in cation deficiency in titanomagnetite (Prevot et al., 1968; Johnson and Melson, 1978; Johnson and Hall, 1978; Akimoto et al., 1984). The remarkable morphological changes that occur during low temperature oxidation are the formation of irregular and curvilinear cracks in the titanomagnetite grains. These cracks were interpreted as the result of change in volume due to the original spinel lattice during oxidation (Larson and Strangway, 1969; Johnson and Hall, 1978; Akimoto et al., 1984). Johnson and Hall have termed them as "shrinkage cracks". Johnson and Hall (1978) have proposed five different stages on the basis of microscopic features associated with progressive low temperature oxidation. The following stages are the proposed low temperature oxidations:

Stage-1: Unoxidised titanomagnetite: Homogeneous titanomagnetite rich in high titanium, free of cracks (unoxidised).

Stage-2: Partial oxidation: The growth of very fine to submicroscopic cracks along the grain boundaries of titanomagnetite is indicated by the change into bright color.

Stage-3: Formation of cracks: Cracks are curvilinear and prominent with the presence of some non-opaque minerals replacing original titanomagnetite towards their grain margins.

Stage-4: Formation of veins: Early formed cracks were filled with silicates and numerous new cracks developed from the earlier cracks as branches. Red pigmentary strain appears growing surrounding the silicates.

Stage-5: Relic grains: Isolated, bright, greyish white relic grains are left after almost complete replacement of titanomagnetite by nonopaque silicate minerals.

Fe-Ti oxide occurs as variable textural associations (Fig. 3.7, 3.8). From the reflected light microscopic study of the sample we have collected, it is evident that the low temperature oxidation of Fe-Ti oxides i.e., Stage-1 is present in the samples from studied area (Fig: 3.10). We get low temperature oxidation of Stage-2(Fig 3.11), Stage-3(Fig 3.12), where curvilinear cracks are developed around the grain boundary and silicate minerals are entering and low temperature oxidation Stage-4(Fig 3.13), where numerous deep cracks are developed from the earlier formed cracks as well as several new cracks are generated.

In some of the studied samples we get pigmentary hematite (Fig 3.14) at places we get the remanent of ultrafine grains of primary magnetite as detritals.

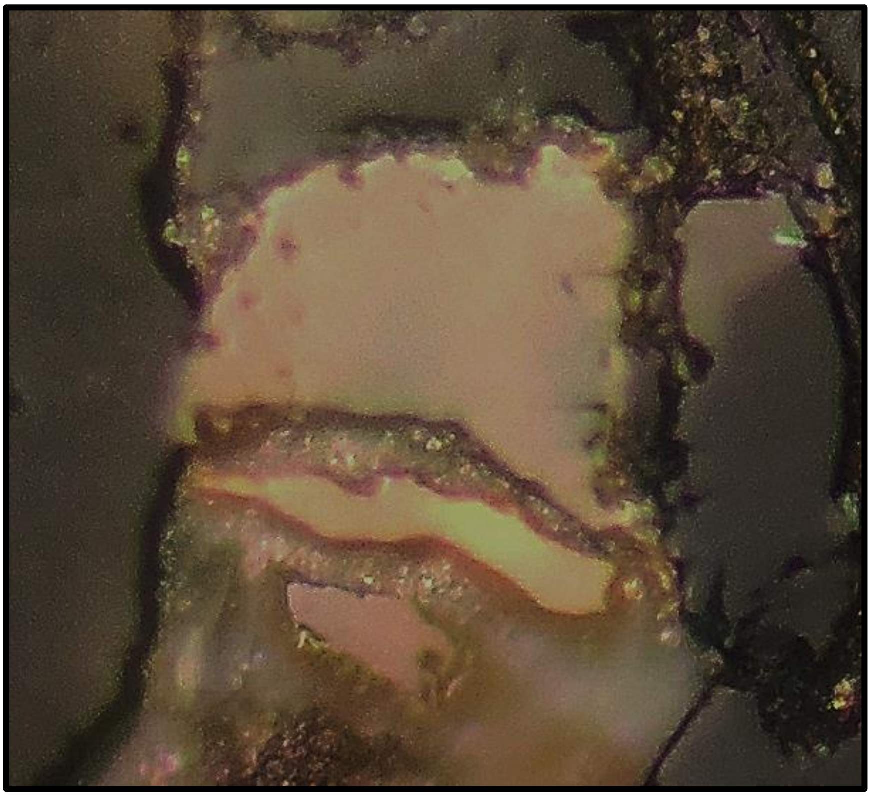

Figure 3.10. Stage-1 of low temperature oxidation present within framework grains (PPL, 500x)

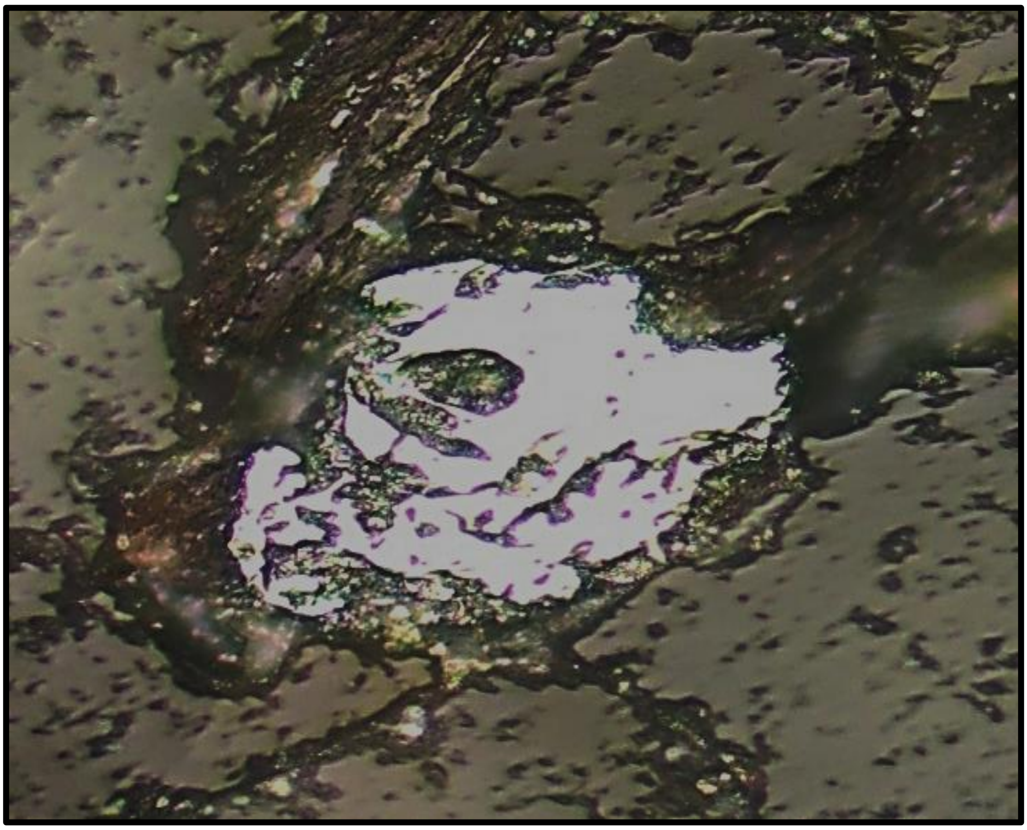

Figure 3.11. Stage-2 of low temperature oxidation (PPL, 100x)

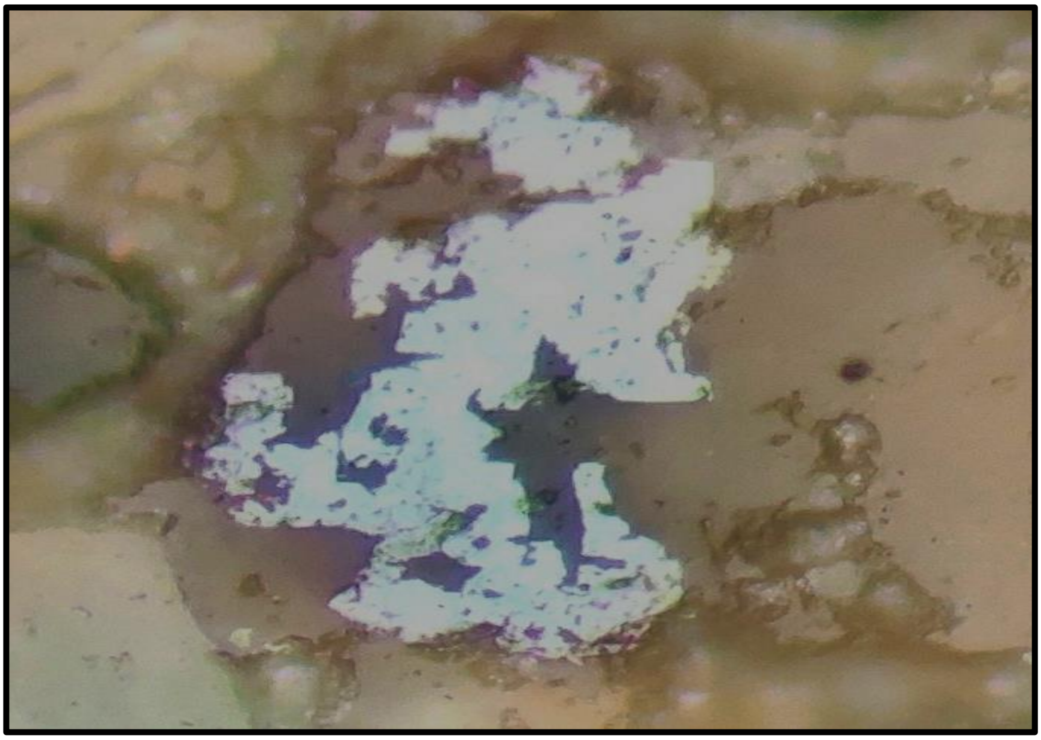

Figure 3.12. Stage-3 of low temperature oxidation (PPL, 100x)

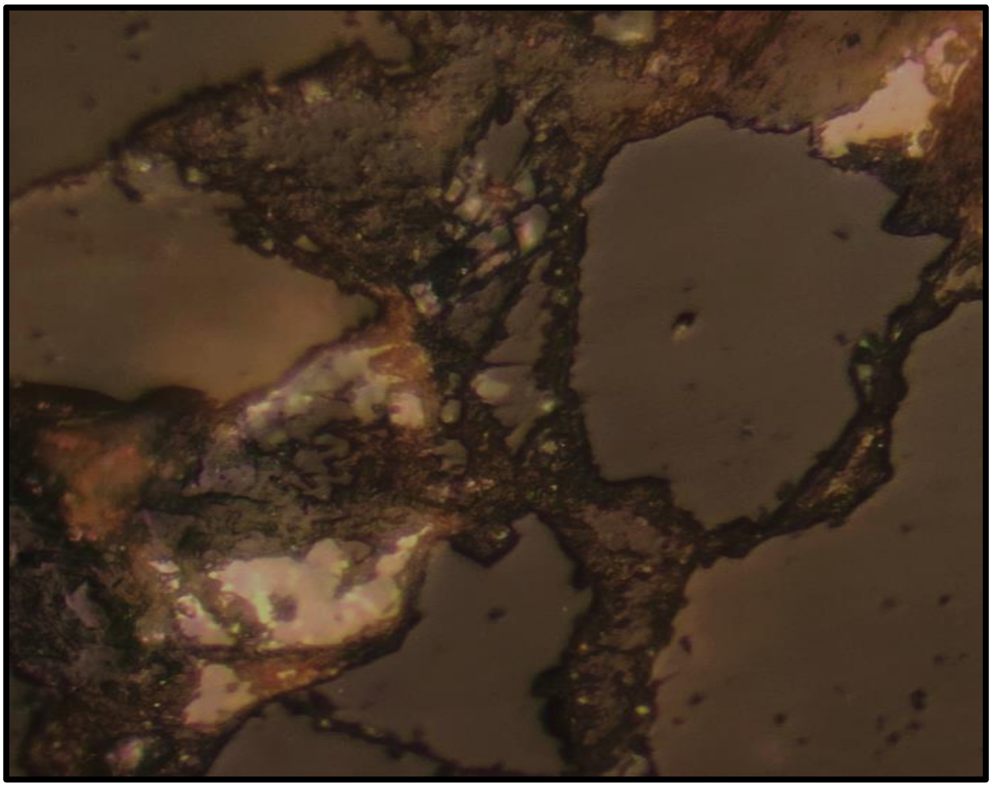

Figure 3.13. Stage-4 of low temperature oxidation (PPL, 100x)

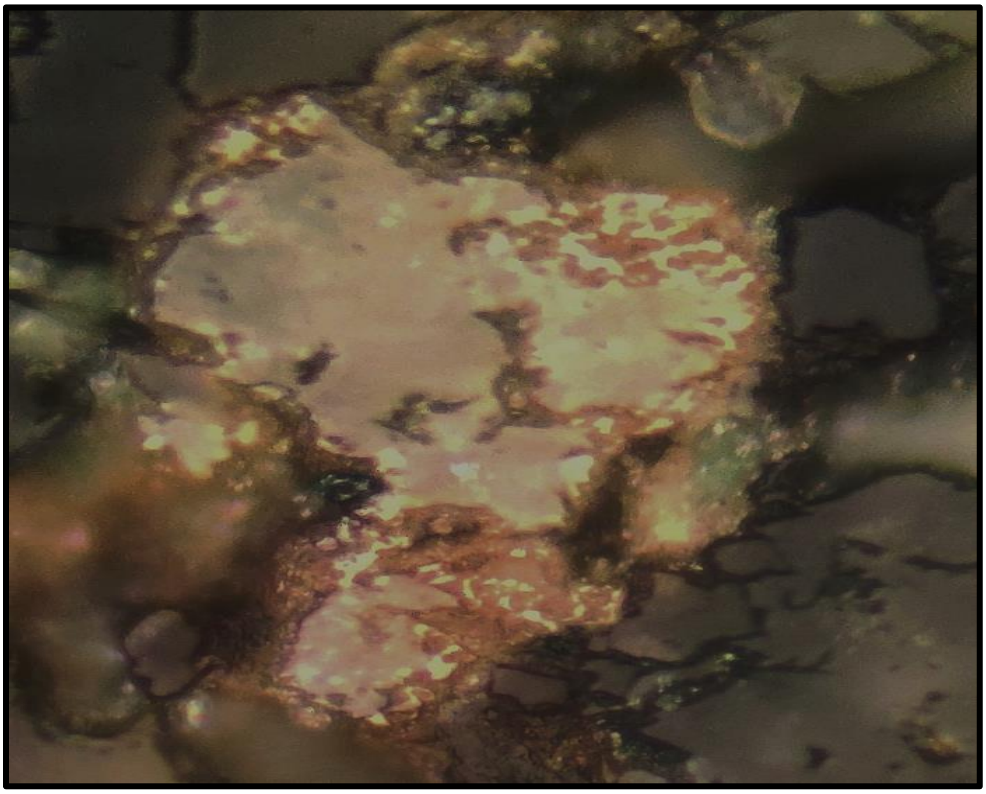

Figure 3.14. Haematite pigmentation (PPL, 100x)

The microscopic study identifies hematite as the predominant opaque oxide occurring as both non-crystalline and crystalline forms in a wide range of grain sizes. The pigmentary hematite, and especially the microcrystalline variety, which is bright red and translucent under transmitted light, is the main contributor to the red colour of the rocks. Relative concentration of pigmentary hematite and hematite microcrystals occur as:

i) **Isolated individual crystals,**

ii) **Secondary growth along silicate grain boundaries,**

iii) **Recrystallized droplets / ultra-fine crystals.**

Neither ilmenite exsolution lamellae nor any signature of exsolution planes of preexisting magnetite crystals have been found along with pigmentary hematites suggesting that the hematite is of low temperature origin. Evidence favours the presence of both detrital and authigenic ultrafine grains of secondary magnetite. The detrital isolated grains of magnetite have often been fractured to form clusters of smaller magnetite grains perhaps resulting from compaction during lithification. Though the original grain boundary is still distinctly recognizable. Due to differential alteration the ultrafine magnetite is observed with widely varying grain sizes even within the samples from a single site. The variability in grain size range of ultrafine magnetite as observed in the collected samples.

The secondary Fe-oxides have developed along the dissolved silicate grain boundaries and also within the reconstituted clay matrix. In some instances, the parent silicate minerals appear to have been removed completely, leaving behind a mixture of authigenic magnetite and altered clay minerals. Occurrence of secondary hematite within the altered biotite grains is a common feature in a number of samples. These grains are usually elongated needle shaped crystals, having developed along biotite cleavage lamellae. Post-depositional late enrichment of iron solution partially or completely surrounds the silicate grains, and also spreads throughout the clay matrix. This also indicates that the rock was highly permeable during the emplacement of the secondary iron solution in the interstitial spaces.

Ultrafine grains of secondary magnetite along the boundary of silicate minerals are found. These ultrafine grains of secondary magnetite are generated from the iron solutions during diagenesis process and the subsequent process of sedimentation.

From the above study we get 3 generations of Fe-Ti oxides.

I. **Detrital primary magnetite**

II. **Pigmentary hematite in the iron solution which is formed by leaching from the iron bearing silicate minerals, mainly biotite.**

III. **Secondary ultrafine grains of magnetite**

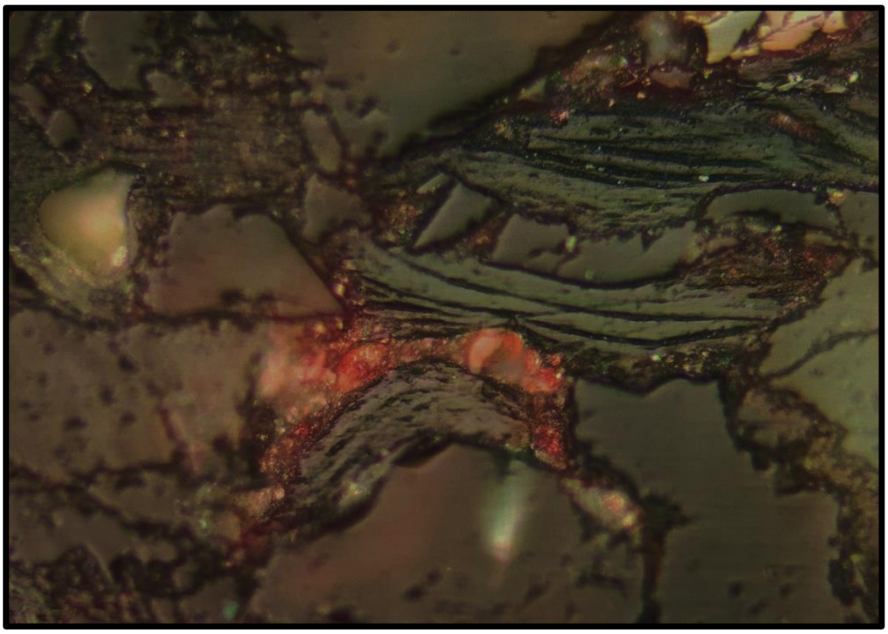

Figure 3.15. Pigmentary hematite solution associated with silicate grains (PPL, 200X)

CHAPTER: 4

ANISOTROPY OF MAGNETIC SUSCEPTIBILITY STUDY

4.1 Introduction:

Anisotropy of susceptibility in minerals i.e., dependence of susceptibility on the direction along which it is measured in a sample, arises from either fundamental anisotropy in the **crystal structure** (**magneto-crystalline anisotropy**) or from non-sphericity of **shape** of mineral particles. The former is a property of all common magnetic minerals, but shape anisotropy due to aligned, elongated particles or to a planar or linear distribution of particles is the most common cause of anisotropy of initial susceptibility observed in rocks. Elongated or platy grains can be aligned for instance by flow in a partially solidified igneous rock or by preferential horizontal settling of platy or elongated grains in sediments. In metamorphic rocks stress is often the aligning agent and a special form of anisotropy may occur termed **textural anisotropy** caused by the occurrence of planes or strings of interacting **magnetic particles**.

Thus, magnetic anisotropy has come to be used as a profitable tool for the detection of rock fabrics, which may not otherwise be apparent.

Shape anisotropy arises from the dependence of demagnetizing factor **N** on particle shape. In an applied field **H**, the effective field, $\mathbf{H_i}$, inside a particle is

$$\boldsymbol{H_i = H - NM}.$$

where **M** is the volume intensity of induced magnetization, **N** is the demagnetizing factor of the particle along the direction of applied field.

$$\boldsymbol{H_i = H - NK_iH_i}$$

$$K_o = \frac{K_i}{(1 + K_i N)}$$

where, Ki and $\mathbf{K_o}$ are the intrinsic and observed susceptibility respectively. The dependence of $\mathbf{K_o}$ on **N** implies variation in $\mathbf{K_o}$ according to the direction in which it is measured in a non-spherical particle. For shape anisotropy to be significant in an elongated particle, $\mathbf{N\ K_i > \sim 0.01}$. This condition is easily met in iron and titano-magnetite minerals, and elongated grains of the latter are the most common cause of the observed anisotropy of initial susceptibility in igneous rocks. In low fields magneto-crystalline anisotropy is not observed in cubic minerals and therefore does not contribute to initial susceptibility anisotropy of rocks, although it does contribute in high field measurements.

In hematite and pyrrhotite, $\mathbf{N\ K_i < \sim 10^{-3}}$ and anisotropy due to the magnetic effect of shape is negligible. However, hematite often occurs in the form of platelets whose crystallographic and easy magnetic axes are in the plane of the particles. Thus there can be susceptibility anisotropy of magneto-crystalline origin in hematite bearing sediments brought about by preferential settling of particles with their planes horizontal or by stress or flow induced alignment in other rocks. In some metamorphic rocks, pyrrhotite particles, also of platy form, are aligned by stress. Quantitatively, anisotropy is conveniently described by the ratio of maximum to minimum susceptibility (**the anisotropy factor**) observed in a rock sample. Typical values are 1.01 – 1.20 in igneous rocks and sediments and up to 2.0 in some markedly structured metamorphic rocks such as scales.

Another aspect of magnetic anisotropy in minerals is its possible influence in deviating from the ambient field direction, the direction of thermo-or chemical remanent magnetization acquired by minerals, thus undermining one of the basic assumptions of palaeomagnetic interpretation. Such a deviation is possible because in an anisotropic mineral the induced magnetization is not in general parallel to the applied field, and TRM or CRM will tend to be acquired along the easy axis (maximum susceptibility) in a particle. This aspect of magnetic anisotropy has been studied by Stacey (1960), Uyeda, Fuller, Belshe and Girdler (1963), Fuller (1963). The deviation of a TRM direction from the ambient field is expected to be rather small (< ~ 5º) in most non-metamorphosed igneous rocks with anisotropy factors not exceeding ~ 1.2, but can be substantial if more marked anisotropy is present.

4.2 Magnetic Fabric:

The susceptibility ellipsoid is triaxial, dimensions defined by the magnitudes of the principal susceptibilities. These lie along three orthogonal axes of symmetry of the ellipsoid and are designated the maximum, intermediate, and minimum susceptibilities $\mathbf{K_{max}}$, $\mathbf{K_{int}}$, and $\mathbf{K_{min}}$. These qualities are combined in various ways to describe different features of the ellipsoid and of the magnetic fabric it represents.

Parameters $\mathbf{P_1}$, $\mathbf{P_2}$, and $\mathbf{P_3}$ are defined by:

$\mathbf{P_1 = K_{max} / K_{int}}$ **= Lineation (L),**

$\mathbf{P_2 = K_{max} / K_{min}}$ **= Anisotropy Factor,**

$\mathbf{P_3 = K_{int} / K_{min}}$ **= Foliation (F).**

L is a measure of the extent of lineation parallel orientation of particles contributing the susceptibility, and **F** of their planar distribution. The ratio $\mathbf{P_3 / P_1}$ is termed the **Eccentricity (E)** of the ellipsoid.

$$E = (Kint)^2 / (K_{max} . K_{min})$$

E > 1, the ellipsoid is **Oblate**, and if $K_{int} \approx K_{max}$, the ellipsoid is **Disc-shaped**. If **E < 1**, the ellipsoid is **Prolate**, and as K_{int} approaches K_{min} the ellipsoid becomes increasingly **Cigar-shaped**. These two ranges of **E** correspond to the dominance of foliation and lineation respectively.

The basic measurements available for analyses of an anisotropy ellipsoid are the susceptibility, **X**, and along its major, intermediate and minimum axes and their orientations.

If crystalline anisotropy can be ignored, as for magnetite, then if the three axes are equal, $X_{max} = X_{int} = X_{min}$, i.e., if the sample is isotropic, these correspond to an average spherical shape for all the grains in the sample. Departure from the average spherical shape can therefore be quantified as the magnitude of anisotropy and the ratios between the three axes can be used to determine whether the shape is predominantly **prolate** (cigar / cylinder shaped) or **oblate** (pancake / disc shaped). **An oblate ellipsoid would be characterized by** $X_{max} \approx X_{int} > X_{min}$**, while a prolate ellipsoid would have** $X_{max} > X_{int} \sim X_{min}$.

The **mean susceptibility**, K_{mean} is given by:

$$(Kmax + Kint + Kmin) / 3$$

4.3 Susceptibility ellipsoids and parameters:

(a) A sphere has equal susceptibility in all directions and hence the axes are undefined and the anisotropy is zero.

(b) The susceptibilities along the three axes are 30.1, 10.1, and 10.0 and are thus clearly prolate, i.e., highly lineated.

(c) The susceptibilities are 30.1, 25.0 and 10.0 i.e., oblate and with a clear foliation.

4.4 METHODOLOGY AND INSTRUMENTS USED FOR MEASURING THE ANISOTROPY OF MAGNETIC SUSCEPTIBILITY:

4.4.1 General Description of the Instrument:

The calculation of Anisotropy of Magnetic Susceptibility involves few simple steps. First of all, the average susceptibility needs to be measured which can be done by the Bartington Susceptibility Meter.

The main laboratory equipment is the MS2 Magnetic Susceptibility Meter. The MS2 Magnetic susceptibility comprises portable measuring instruments, the MS2 meter and a variety of sensors. The MS2 circuitry is housed in a sealed enclosure weighing 1.2 kg (2.6 lb) with approximate dimensions of 260 mm x 158 mm x 50 mm (10 inch x 6 inch x 2 inch). The operating switches a TNC sensor cable connector and a four-digit LCD are situated on the front panel. Each sensor is designed for a specific application and sample type and is connected to the MS2 meter via a sample coaxial cable. The meter displays the magnetic susceptibility value of materials when these are brought within the influence of the sensor. An RS 232 serial interface allows the instrument to operate in conjunction with custom software running on a portable data logger or PC. The MS2 meter is powered by internal chargeable batteries. Internal Ni-Cd batteries provide 8 hours' continuous use and can be recharged from either the mains or a vehicle dashboard. The circuits within the MS2 powers the sensors and processes the measurements information produced by them. An instrument stand is provided for laboratory use and a carrying bag is supplied for field portability.

The measurements are obtained digitally using a time dependent method. This results in precise and repeatable measurements. The sensors are independently calibrated and are therefore fully interchangeable between MS2 instruments. The range of sensors measurements of individual laboratory soil and rock samples, sediment cores, soil surface, rock exposures or down auger holes.

Data Processing:

The following software is available in the laboratory for data processing:

- **MULTISUS**: This window software runs on user's PC and provides data capture from the MS 2 Meter, via the RS 232 serial port, when used with the MS2B, MS2C, MS2E,MS2G, MS2H sensors when used with MS2 B sensors the program allows volume or mass specific susceptibility measurements with correction for sample volume or mass where appropriate, and calculation of the coefficient of frequency dependent susceptibility when used in conjunction with the MS2 C, correction for the ratio of core to sensor diameter can be automatically applied. The software offers baseline drift correction for all the above sensors.
- **AMSWIN-BAR**: This Windows programme permits the measurement of the anisotropy of magnetic susceptibility. Sample adapters are provided with the software.
- **AMS2**: The latest version of AMS BAR is an interactive environment for measuring Magnetic Susceptibility Anisotropy, Calculating the principle components of the Fabric ellipsoids for a single specimen, and providing a summary of the principle components and their associated errors for a group of samples. The AMS2 software has been specifically designed for Bartington instrument MS2 Susceptibility meter with a 36mm sensing coil using an IBM PC (or true compatible) micro computer running under MSDOS 2x or greater, for standard 25mm diameter paleo-magnetic specimens.

4.4.3 Principles of Operation:

The magnetic state of a specimen is generally described by the following equation.

$$\boldsymbol{B} = \mu_0(\boldsymbol{H} + \boldsymbol{M})$$

Where B=Flux density of the specimen in TESLA (T)

μ_0 is the permeability of free space N/A^2. This is a constant (4π x 10-7), and the applied field strength in A/m. Dividing the above equation by H we get ,

$$\mu = \mu_0 + \mu_0 \boldsymbol{k}$$

where k= volume magnetic susceptibility of the specimen(Dimensionless)

Rearranging we get,

$$\mu_0 \boldsymbol{k} = \mu - \mu_0$$

The MS2 instrument measures the Magnetic Susceptibility in the following way. The sensor consists of a very high thermal stability oscillator for which a wound indicator is the principle frequency determining component. When the indicator contains only air the value of μ_0 determines the frequency of oscillation.

When the indicator is placed within the influence of the specimen to be measured the value of μ determines the frequency of oscillation. The meter to which the sensor is connected digitize the μ_0 and μ dependent frequency values with a resolution of better than 1part in a million computes the value of magnetic susceptibility.

The value of μ_0 is constant but the variable of interest is relatively small. Therefore, a thermally induced sensor drift needs to be eliminated by occasionally obtaining a new 'air' value (to re-establish the μ0 reference by depressing the zero button on the MS2 meter.) The μ value is obtained by pressing the measure button. The magnetic susceptibility value is displayed digitally and output via a serial interface.

4.5 USEFULNESS OF AMS STUDY IN SEDIMENTARY ROCKS:

If mineral grains have a shape of crystalline anisotropy and their magnetic properties will vary with direction if these grains are aligned by:

a) Current flow during deposition (in sediments) can be established i.e. paleo-current direction of sedimentary basin should be determined.

b) The studied rocks will have anisotropic magnetic properties. Thus AMS is a rapid indicator for fabric where other methods of determinations are usually laborious.

The results from the Anisotropy Susceptibility measurements and ellipsoid calculations by AMS-BAR software of the studied rock cores of my field area reveal that the eccentricity is greater than 1, i.e getting oblate ellipsoid which implies that the minerals responsible for magnetic susceptibility are aligned along the foliation present in the rock which is defined mainly by plagioclase grains.

The results from the anisotropy of the magnetic susceptibility measurements and ellipsoid calculation by AMS-BAR software of the studies rocks are shown in the following table.

Table. 4.1. Database containing the AMS parameters used in the present study

K1(D/I)	K2(D/I)	K3(D/I)	Km	F	L	P	T	q-Factor
343.1/30.6	251.0/3.6	154.9/59.2	9.2	1.1	1.3	1.48	-0.42	0.46
268.4/84.1	161.5/1.7	71.4/5.6	22.5	1.1	1.2	1.29	0.24	0.22
107.2/21.3	198.5/3.5	297.5/68.5	14.8	1.2	1.1	1.29	0.24	0.36

352.2/44.7	196.2/42.7	94.6/12.3	5.4	1.2	1.2	1.45	0.09	0.11
53.9/0.8	144.3/23.2	322.1/66.7	23.9	1.2	1.1	1.33	0.01	0.2
264.8/36.4	147.9/31.6	29.5/37.7	20	1.3	1.2	1.44	0.29	0.52
267.0/67.8	136.4/14.9	42.0/16.1	4.9	1.3	1.3	1.73	-0.05	1.2
252.1/39.1	154.0/9.8	52.5/49.2	11.3	1.0	1.5	1.64	-0.09	0.14
307.4/1.0	216.4/43.3	38.5/46.7	8.3	1.1	1.3	1.42	-0.45	0.91
333.1/15.2	232.7/28.3	86.1/57.1	8.4	1.1	1.1	1.26	-0.24	0.72
178.7/11.8	44.1/73.1	271.3/11.8	1.5	5.3	1.8	39.25	0.58	1.04

4.6 Plotting of AMS data:

4.6.1 K_m versus P_j plot :

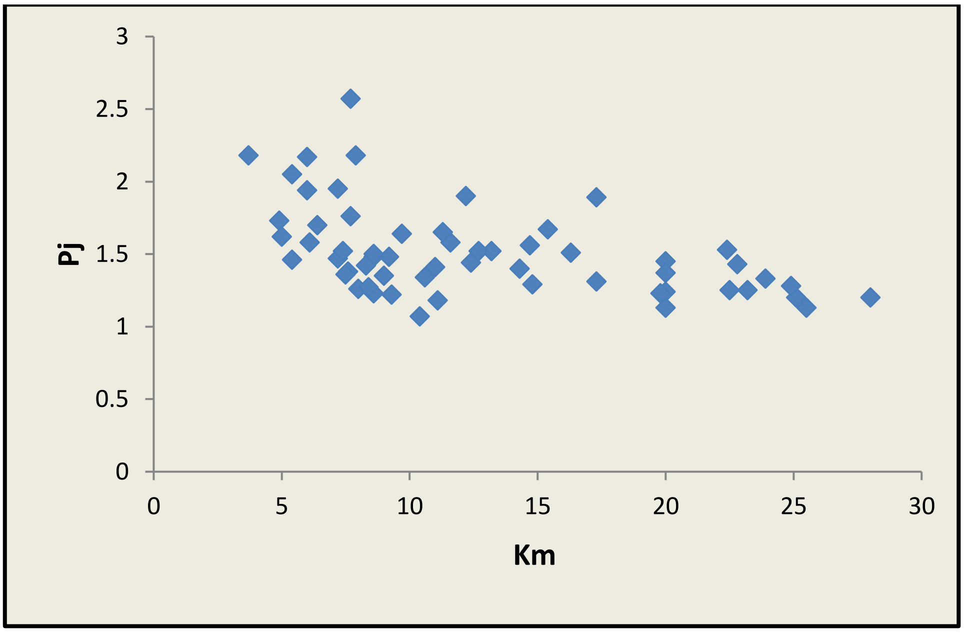

Figure 4.1. K_m versus P_j plot for the studied rocks

- Mean susceptibility (K_m) = (K_1 + K_2 + K_3) / 3

- Anisotropy degree (P_j) = $\exp^2\sqrt{(\eta_1 - \eta_m)^2 + (\eta_2 - \eta_m)^2 + (\eta_3 - \eta_m)2}$ (Jelinek, 1981)

<u>The following interpretation can be done from Km-Pj plots:</u>

There is a negative correlation between the two parameters. With increase in the mean susceptibility, magnetic anisotropy decreases. This means that the mean susceptibility is not controlling the magnetic fabrics. Thus, the mineralogy has no effect. The anisotropy detected in the study is purely orientational. Thus, the rocks are suitable for paleo-current analysis.

4.6.2 JELINEK PLOTS :

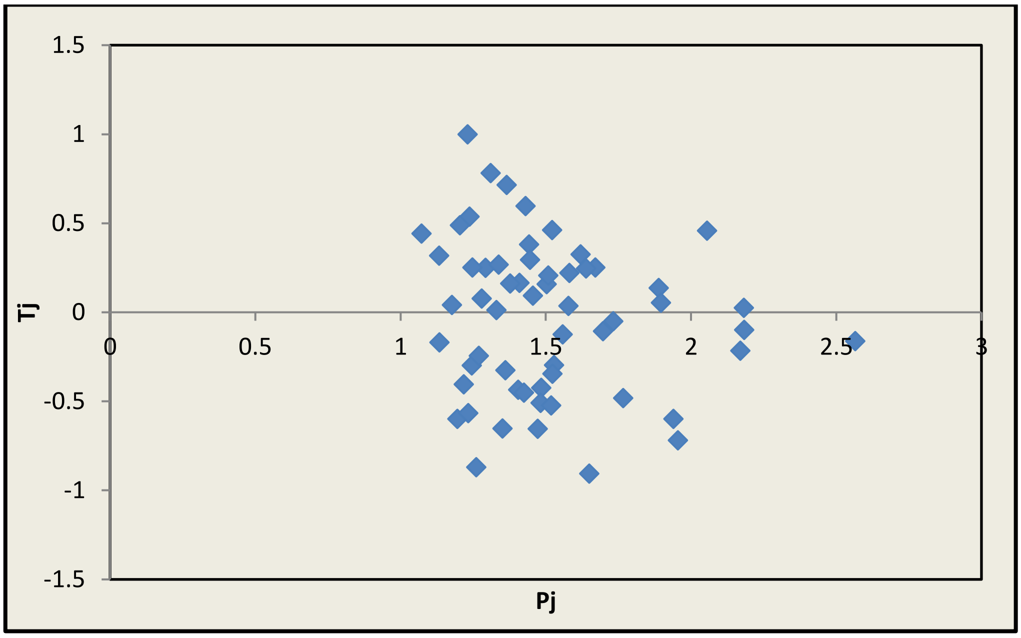

Figure 4.2. P_j versus T_j plot for the studied rocks

- **Shape factor (T) = ($2\eta_2 - \eta_1 - \eta_3$) / ($\eta_1 - \eta_3$)**
- **Anisotropy degree (P_j) = $\exp^2\sqrt{(\eta_1 - \eta_m)^2 + (\eta_2 - \eta_m)^2 + (\eta_3 - \eta_m)2}$ (Jelinek, 1981)**

Following interpretation can be done from the Jelinek plots:

Subequal amount of oblate and prolate grains are found. Prolate grains mainly contribute to the sedimentological anisotropy studies as the scope of this study. Prolate grains are responsible for recording the anisotropy degrees in preferred directions. Oblate grains lack such capability because of the equality in their principle susceptibility axes. The prolate grains have their maximum susceptibility axes aligned parallel to the flow direction thereby preserving its trend. This is also evident from the fact that the prolate grains have relatively higher degree of anisotropy. The Pj value is almost constant as evident from the graph. Constant low Pj value depicts lesser degrees of anisotropy which further points towards high energy environment leaving a isotropic component of magnetic fabrics.

4.6.3 STEREO PLOTS:

4.6.3.a Plotting all the K value on a single stereogram:

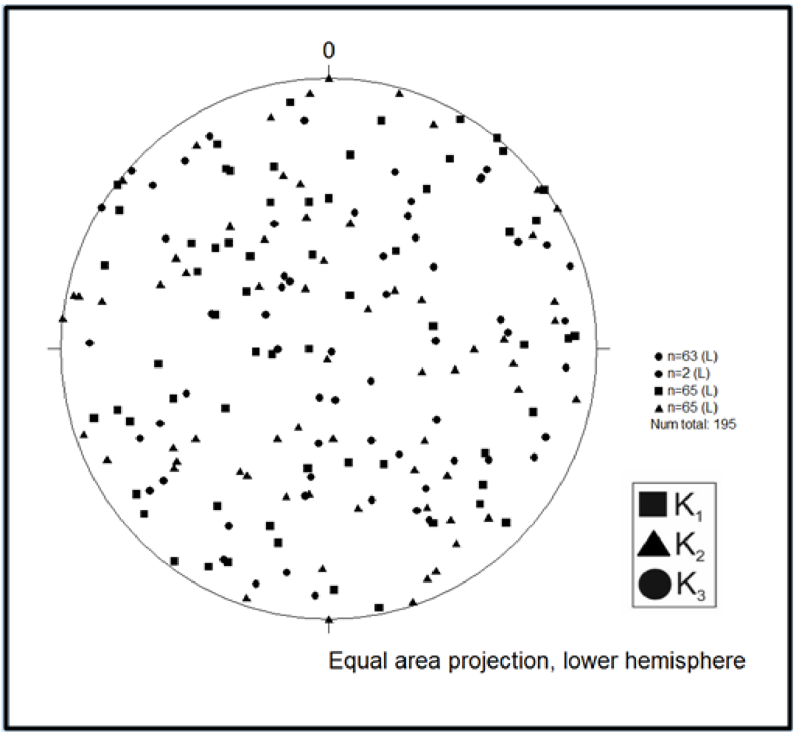

Figure 4.3. Stereo plot for the principle susceptibility axes plot for the studied rocks

Implications from Stereo plot:

There is a overall scattering in the principle susceptibility axes. This depicts that the depositional current for these lower Gondwana rocks was much weaker. This failed to develop strong anisotropy in the rocks; depicted by the lower values for the degrees of anisotropy. The maximum and the intermediate susceptibility axes have tendencies to disperse about the periphery pointing towards horizontal plane of sedimentary deposition. Thereby the nature of the grains is mainly oblate. However, overall suitability of the data for paleo-current analysis can be judged from mathematical plots.

4.6.3.b ROSE DIAGRAM:

The Eigen values that are obtained during the AMS study were plotted in the Circular Diagram with the help of STEREO software. Based on the intensity of the maximum, minimum and the intermediate values of the Eigen values on the circular diagram they are classified into two categories which may be termed as STRONG CLUSTER and WEAK CLUSTER. The magnetic foliation planes are constructed through the plots of the maximum and the intermediate Eigen value plots the same software. Based on the variation attitude of this magnetic foliation planes the stereo diagrams can be classified into two types which are called STRONG GIRDLE and WEAK GIRDLE.

Implications from Rose diagram:

The flow has almost 360-degree orientations. This has also acquaintance with the nature of the foliation plane and sedimentary grains. However, three strong channels are evident in NE, NW and WSW directions. Environmental implications suggest that the environment was strongly fluvial with glacial influxes. 360-degree orientation of the axes also suggest oblate grains. Multidirectional of the paleo-current also replicated by more than one orientation of the lath shaped mica grains. Overall environment was not calm and quite which is also earlier established based on primary structure studies.

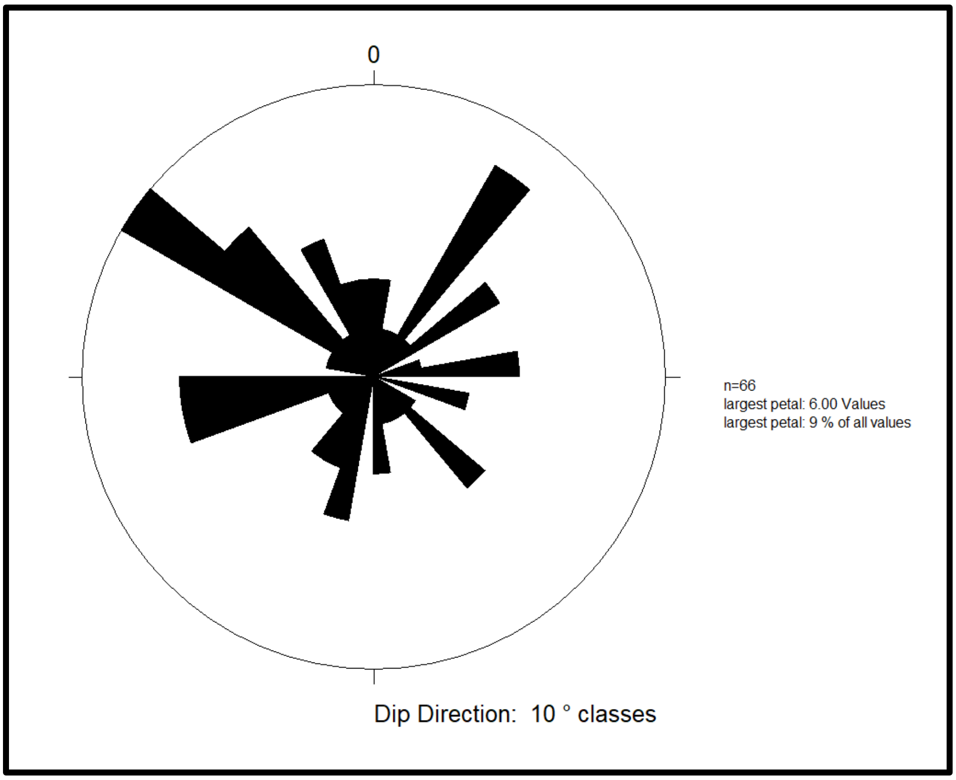

Figure 4.4. Rose diagram for the maximum susceptibility axes (paleo-current) plot for the studied rocks

CHAPTER: 5

RESULTS AND DISCUSSIONS

The nature of the magnetic fabrics in the studied units of the the Talchir and Barakar Formations in the Damodar Valley seems to be primary with some local disturbances. Because of the similarity of the values of AMS parameters in the Talchir and Barakar Formations, the general nature of the magnetic fabrics in both the formation are discussed under the same heading.

The distribution patterns of the principal susceptibility axes in the equal area diagrams are evidences for the same. Although it is observed that the principal susceptibility axes are slightly dispersed rather than clusters, the average trend of the magnetic foliation planes can be identified from the lower hemisphere equal area diagrams. The plots of the maximum and intermediate susceptibility axes are found over here to be near the periphery which signifies low dips of the magnetic foliation plane and thus the nature of the magnetic fabric is pointed towards an oblate one in both the units. The plots on P_j versus T diagram are dominantly over the oblate field which corroborates the contention. However, there are a considerable number of plots in the prolate field too, which, of course needs explanation. The ideal condition for the development of an oblate fabric is a calm and quite (still water) sedimentary environment where there is absence of currents which can disrupt the perfect oblateness of the magnetic fabric (Tarling and Hrouda, 1993). However, the sedimentary environments that prevailed during the deposition of these two units were not calm enough to develop a strict oblate fabric. The Talchir formation was deposited in a Glacio-fluvial environment (Dutta, 2002; Suttner and Dutta, 1986), also, with some stormy events and open marine storm surges evident from various primary sedimentary features, especially, sole marks (Bhattacharya et al., 2004; Bhattacharya and Bhattacharya, 2015). Thus, the magnetic grains (ferro-, para- or dia-magnetic) over here in this unit, which contributes towards the susceptibility and its anisotropy, were not deposited in the basin only due to gravitational settling. There were effects of other sedimentary environmental factors. Consequently, although a predominant oblate fabric prevailed parallel or sub-parallel to the bedding there has developed a superimposing lineation impinging a degree of prolateness in the fabric. Such natures of magnetic fabrics are generally supported by the presence of slump structures (Tarling and Hrouda, 1993) which are abundant in the hummocky cross stratifications of the Talchir Formation. In case of the Barakar Formation, the explanation of the magnetic fabrics needs some other environmental explanation. The Barakar sediments were deposited in a fluvial environment (braided to meandering) with ample evidences of channel shifting and accretion of point bar (Dutta, 2002; Ghosh, 2002; Suttner and Dutta, 1986; Casshyap and Tewari, 1987; Bhattacharya et al., 2016). The randomness noticed in the orientations of the principal susceptibility axes in the Barakar Formation can thus be attributed towards the presence of a number of channels migrating events. However, similar degrees of prolateness were observed in the fabrics of Barakar Formation similar to Talchir, which has similar explanations too i.e. the environment of deposition in Barakar Formation was also not a still water one which prevents the development of an ideal oblate fabric and impinges a deviation towards prolate fabric therein.

The first and foremost criterion which is required for paleocurrent analysis using AMS data is that the rock unit must preserve its original primary (depositional) fabric. The values of q-factor in the studied sections served for the same. Thus, in spite of the dispersion (rather than clusters) depicted by the principal susceptibility axes, their orientations are controlled by primary depositional factors and the imbrication of K_1 (maximum) axes can be treated as the paleocurrent directions for both Talchir and Barakar Formations. The paleocurrent pattern in the available literature and are quoted herein in the text. The rose diagram for the imbrication described by the K_1 axes as an indication of the paleocurrent direction. From the figures, it is observed that the paleocurrent patterns both in the Barakar and Talchir Formations are due NE, NW and S dominantly. The higher values of the degrees of anisotropy (P_j) in Talchir supports for the same. Thus, the current strength was more in the Talchir Formation (Glacial with marine surges) is more than that in Barakar Formation (braided to meandering channels). The paleocurrent patterns thus obtained from the AMS data thus bears a strong analogy with those earlier obtained from the same rock units using sedimentological methods (Suttner and Dutta, 1986; Dutta, 2002; Ghosh, 2002; Bhattacharya et al., 2004; Bhattacharya and Bhattacharya, 2015). There is a very prominent orientation of the K_1 axes all throughout 360 degrees of the diagram, although very few in number. This is basically due to the strongly oblate shaped grains which remained unaffected by the currents and settled in the sedimentary basin exclusively by gravitational settling. The same inference can be drawn from the orientations of the biotite laths with are strongly imbricated in the Talchir Formation and are relatively random in the samples from Barakar Formation.

CHAPTER: 6

CONCLUSIONS

From the present study, it can be concluded that the application of AMS in sedimentary basins can be used into two categories: (a) Robustness of AMS as a supporting tool in understanding the depositional sedimentary environments and paleocurrent patterns in basin analysis studies, (b) Patterns of paleocurrent and their correlation with the depositional environment from the Barakar and Talchir Formations in the Damodar Valley.

First, it is well established from the present case study that AMS is a powerful tool in paleocurrent and sedimentary environment analysis as it has the capability of recording any minimum changes in directional attributes viz. current direction. The nature of variation of the orientations of the susceptibility axes also have strong implication towards changes in the depositional environment. similar AMS data variations and changes can also be shown by rocks of multiply deformed terrain where the magnetic fabric elements have no primary (depositional or paleocurrent related) significances. Thus, it is strongly recommended to define the genesis of the magnetic fabrics (depositional or tectonic) before using them as proxies for sedimentological characteristics by calculating the values of q-factor.

Secondly, the application of AMS study in sedimentary environment and paleocurrent analysis proved its usefulness in the present study. The magnetic fabrics observed in the Lower Gondwana successions are primary and are developed during the deposition of the sediments in the concerned environment. Both the nature of the magnetic fabrics within the studied section and the paleocurrent patterns have strong accordance with the sedimentary environment discussed in available literature. The results from the various AMS parameters and the distribution of the principal susceptibility axes over the lower hemisphere equal area diagram supports for the same.

REFERENCES:

Baas JH, Hailwood EA, McCaffrey WD, Kay M, Jones R (2007) Directional petrological characterization of deep-marine sandstones using grain fabric and permeability anisotropy: Methodologies, theory, application and suggestions for integration Earth Sci. Rev.82:101–142.

Bakhtari HR, Dominique FL, Charles A, Jamshid H (1998) Magnetic fabrics of Tertiary sandstones from the Arc of Fars (Eastern Zagros, Iran). Tectonophys 284: 299–316.

Basavaiah N, Appel E, Lakshmi BV, Deenadayalan K, Satyanarayana KVV, Misra S, Juyal N, Malik MA (2010) Revised magnetostratigraphy and characteristics of the fluviolacustrine sedimentation of the Kashmir basin, India, during Pliocene-Pliestocene. J. Geophys. Res. 115: B08105.

Bhattacharya B, Bhattacharjee J, Banerjee S, Bandyopadhyay S, Das R (2016) Seismites in Permian Barakar Formation, Raniganj Basin, India: implications on Lower Gondwana basin evolution. Arab J Geosci. 9: 300.

Bhattacharya HN, Bhattacharya B (2015) Lithofacies architecture and paleogeography of late Paleozoic glaciomarine Talchir Formation, Raniganj Basin, India. J Paleogeogr. 4: 269–283.

Bhattacharya HN, Bhattacharya B, Chakraborty I, Chakraborty A, (2004) Sole marks in storm event beds in the Permo-Carboniferous Talchir Formation, Raniganj Basin, India. Sedimentary Geology, 166(3-4), 209-222.

Blasley JR, Buddington AF (1960) Magnetic susceptibility anisotropy and fabric of some Adirondack granites and orthogenesis. Am. J. Sci. 258A: 6-20.

Ca˜n´on-Tapia E (2000) The anisotropy of magnetic susceptibility of lava flows: An experimental approach. J. Volcanol. Geotherm. Res. 98:219–233.

Casshyap SM, Tewari RC (1987) Depositional models and tectonic evolution of Gondwana basins. The Palaeobotanist 36: 214-229.

Chatterjee S, Gain D, Mondal S (2016) Magneto Mineralogy Characterization and Analysis of Magnetic Fabrics of the High-Grade Rocks from Chilka Lake Area, Eastern Ghats Belt, India. Earth Sci.India 9(I): 29-47.

Chatterjee S, Mondal S, Gain D, Baidya TK, Mazumdar D (2018b) Interpretation of magnetic fabrics in the Dalma volcanic rocks and associated meta-sediments of the Singhbhum mobile Belt. J. Earth Syst. Sci. xx: xxx-xxx.

Chatterjee S, Mondal S, Roy B, Gain D (2017) Magnetic Fabric As A Tool To Determine Kinematic Vorticity number of The High-Grade Rocks From Chilka Lake Area, Eastern Ghats Belts, India. Int J Recent Sci Res.8(6): 17845-17850.

Chatterjee S, Mondal S, Roy P, Gain D, Bhattacharya A (2018a) Magneto-mineralogical characterization andmanifestations magnetic fabrics from thegneissic rocks and associated intrusive bodiesin and around Bankura and Purulia Districts,West Bengal. Curr. Sci. 114(x): xxx-xxx.

Das AK, Piper JDA, Bandopadhyay G, Mallick SB, Sherwood, GJ, Mondal S (1999) Magnetopetrologic Study of Sediments of the Gondwana Supergroup, Northeast India. Mem. Geol. Soc. India 44: 117-127.

Dutta P (2002) Gondwana Lithostratigraphy of Peninsular India. Gondwana Research (Gondwana Newsletter Section) 5:540-553.

Dutta PK (1987) Upper Kamthi: a riddle in the Gondwana stratigraphy of Peninsular India. In: McKenzie, G.D. (Ed.), Geophysical monograph 41. Amer. Geophys. Union 229-238.

Dutta PK (1997) Interpreting glacial climate from detrital minerals in sediments. In: Martini, 1.P (Ed.), Late glacial and postglacial environmental changes. Oxford University Press.

Ellwood BB (1980) Application of the anisotropy of magnetic susceptibility method as an indicator of bottom water flow direction. Mar. Geol. 34: 83–90.

Ellwood BB, Crick RE (1988) Paleomagnetism of Paleozoic asphaltic deposits in Southern Oklahoma, USA. Geophys. Res. Lett. 15: 436-439.

Ernst RE, Baragar WRA (1992) Evidence from magnetic fabric for the flow pattern of magma in the Mackenzie giant radiant dyke swarm. Nature 356: 511–513.

Ghosh PK, Mitra ND (1975) History of Talchir sedimentation in Damodar valley basins. Geol. Surv. India Mem. 105: 1-117.

Ghosh SC (2002) The Raniganj Coal Basin: an example of an Indian Gondwana rift. Sedimentary Geology 147: 155–176.

Ghosh SC, Nandi A, Ahmed G, Roy DK (1996) Study of Permo–Triassic boundary in Gondwana sequence of Raniganj Basin. Proc. IXth International Gondwana Symposium. Oxford and IBH Pub., New Delhi, Calcutta: 195–206.

Gibbs AD (1984) Structural evolution of extensional basin margins. J. Geol. Soc. (London) 141: 609–620.

Graham JW (1954) Magnetic susceptibility anisotropy, an unexploited petrofabric element. Geol. Soc. Am. Bull. 65:1257–1258.

Graham JW (1966) Significance of magnetic anisotropy in Appalachain sedimentary rocks. Am. Geophys. Union Mongor 10: 627-48.

Granar L (1958) Magnetic measurements on Swedish varved sediments. Arkiv. F. Geofysik 3: 1-40.

Hamilton N, Rees AI (1970) The use of magnetic fabric in paleocurrent estimation; In: Paleogeophysics (ed.) Runcorn S K (London: Academic Press): 445–464.

Hrouda F (1982) Magnetic anisotropy of rocks and its application in geology and geophysics. Geophys. Surveys 5: 37-82.

Ising G (1942) On the magnetic properties of varved clay. Ark. Mat.Astr. Phys.29:1–37.

Jackson MJ (1991) Anisotropy of magnetic remanence a brief review of mineralogical sources, physical origins and geological applications, and comparison with susceptibility anisotropy. Pure Appl. Geophys.136:1–28.

Jelinek V (1981) Characterization of the magnetic fabric of rocks. Tectonophysics 79: T63 T67.

Jelínek, V (1978) Statistical processing of magnetic susceptibility measured on groups of specimens. Stud. Geophys. Geod. 22: 50–62.

King RF (1955) The remnant magnetization of artificially deposited sediments. Mon. Not. R. Astr. Soc. 7: 115-134.

Knight MD, Walker GPL (1988) Magma flow directions in Dikes of the Koolau Complex, Oahu, determined from magnetic fabric studies. J. Geophys. Res.93(B5): 4301–4319.

Liu B, Saito Y, Yamazaki T, Abdeldayem A, Oda H, Hori K, Zhao Q (2001) Paleocurrent analysis for late Pleistocene–Holocene incised-valley fill of the Yangtze delta, China by using anisotropy of magnetic susceptibility data. Mar. Geol.176: 175–189.

Lowrie W, Hirt AM (1987) Anisotropy of magnetic susceptibility in the Scaglia Rossa pelagic limestone. Earth Planet Sci. Lett.82: 349–356.

Mazumdar SK (1988) Crustal evolution of the Chotanagpur gneissic complex and the mica belt of Bihar. In: Mukhopadhyay, D.(Ed.), Precambrian of the Eastern Indian Shield. Geol. Soc. India, Mem. 8: 49–83.

Mondal S, Mazumdar D, Chatterjee S, Gain D, Shil R (2017) Nature of flow patterns of Rajahmundry lava,Gowripatnam area, West Godavari, India:Insights from AMS studies. Curr. Sci. 113(9): 1719-1728.

Nagata T (1961) Rock magnetism, Maruzen, Tokyo.

Papanna G, Venkateshwarlu M, Periasamy V and Nagendra R (2014) Anisotropy of magnetic susceptibility (AMS) studies of Campanian–Maastrichtian sediments of Ariyalur Group, Cauvery Basin, Tamil Nadu, India: An appraisal to Paleocurrent directions. J. Earth Syst. Sci. 123(2): 351–364.

Par´es JM, Hassold NJC, Rea DK, van der Pluijm BA (2007) Paleocurrent directions from paleomagnetic reorientation of magnetic fabrics in deep-sea sediments at the Antarctic peninsula Pacific margin (ODP Sites 1095, 1101).Mar. Geol.242: 261–269.

Parés J.M., van der Pluijm B, Dinare`s-Turell, J (1999) Evolution of magnetic fabrics during incipient deformation of mudrocks (Pyrenees, northern Spain). Tectonophysics 307: 1 –14.

Park CK, Doh SJ, Suk DW, Kim KH (2000) Sedimentary fabric on deep-sea sediments from KODOS area in the Eastern pacific. Mar. Geol.171: 115–126.

Piper JDA, Elliot MT, Kneller BC (1996) Anisotropy of magnetic susceptibility in a Paleozoic Flysch basin: The Windermere Supergroup, northern England.; Sedim. Geol.106: 235–258.

Potter PE, Maynard JB, Pryoy WA (1980) Sedimentology of Shale. Springer Verlag, Heidelberg.

Potter PE, Pettijohn, FJ (1977) Paleocurrents and Basin Analysis. Academic Press, New York.

Raja Rao, C.S. (Ed.), (1987) Coalfields of India. Bull. Geol. Surv. India, Ser. A, vol. 45, IV. Part I, Geological Survey of India Publication, Calcutta 1–247.

Rathi G, Sangode SJ, Kumar R, Ghosh SK (2007) Magnetic fabrics under high-energy fluvial regime of the Himalayan Foreland Basin, NW Himalaya. Curr. Sci. 92(7): 933–944.

Rees AI (1961) The effect of water current in the magnetic remanence and anisotropy of susceptibility of some sediments. Geophys. J.5: 235–251.

Rochette P, Jackson M, Aubourg C (1992) Rock magnetism and the interpretation of anisotropy of magnetic susceptibility. Rev. Geophys.30:209–226.

Sangode SJ (2001) Application of magnetic fabric studies in an ancient fluvial sequence of NW Himalaya. Curr. Sci.81(1)**:** 66–71.

Schieber J, Ellwood BB (1988) The coincidence of macroscopic paleocurrent indicators and magnetic lineation in shales from the Precambrian belt basin. J. Sedim. Petrol. 58(5): 830-835.

Schieber J,Ellwood BB (1993) Determination of basin wide paleocurrent patterns in a shale succession from anisotropy of magnetic susceptibility (AMS): A case study of the Mid-Proterozoic Newland Formation, Montana J. Sedim. Petrol.63: 878–880.

Sinha S, Sen K, Sangode SJ, Kumar R, Ghosh, SK (2009) Sedimentology and magnetic fabric studies of Mio-Pliocene fluvial succession in the NW Himalayan foreland basin. Curr. Sci, 96(2): 260-267.

Stacey FD, Joplin G, Lindsay J (1960) Magnetic anisotropy and fabric of some foliated rocks from S.E. Australia. Geophysica Pura Appl. 47: 30-40.

Suttner LJ, Dutta PK. (1986) Alluvial sandstone composition and paleoclimate: I. Framework mineralogy. J. Sediment. Petrol. 56 (3): 329–345.

Taira A (1989) Magnetic fabric and depositional processes in sedimentary facies in the Active Plate Margin, Tokyo. Terra Scientific Publishing.

Tarling DH, Hrouda F (1993) The Magnetic Anisotropy of Rocks. Chapman and Hall, London.

Veloso EE, Anma R, Ota T, Komiya T, Kahashuma S,Yamazaki T (2007) Paleocurrent patterns of the sedimentary sequence of the aitao ophiolite constrained by anisotropy of magnetic susceptibility and paleomagnetic analysis. Sedim. Geol. 201:446–460.